Multicomponent Polymer Systems: Polymer Compositional Analysis using Low-Field ^{1}H-NMR Spectroscopy and Tuning the Compositional Drift in Styrene/Isoprene Anionic Copolymerizations

by

Sneha Bukkapatna Chakrapani

A thesis submitted to the Graduate Faculty of
Auburn University
in partial fulfillment of the
requirements for the Degree of
Master of Science

Auburn, Alabama
May 4, 2019

Keywords: ^{1}H-NMR Spectroscopy, Anionic Copolymerization, Compositional Drift, Reactivity Ratios

Approved by

Dr. Bryan Beckingham, Chair, Assistant Professor, Department of Chemical Engineering
Dr. Maria Auad, Professor & Director, Center for Polymer and Advanced Composites
Dr. Andrew Adamczyk, Assistant Professor, Department of Chemical Engineering

ABSTRACT

This Thesis investigates multicomponent polymer systems in the context of their characterization and their synthesis. The composition of the different polymers comprising multicomponent polymer systems is a vital variable in tuning their properties. Herein, low-field ^{1}H NMR Spectroscopy (60 MHz), a newly commercially available technology, is inspected as a possible low-cost alternative to the significantly more expensive (in terms of capital and maintenance costs) higher-field NMR spectrometers (> 250 MHz) for the compositional analysis of multicomponent polymer systems, namely polymer blends and block copolymers. The results from a low-field spectrometer are corroborated using a high-field spectrometer and are found to be adequately quantitative within the typical confidence for compositional analyses of this nature using traditional high-field NMR spectroscopy. Next, a series of copolymers of styrene and isoprene are synthesized by anionic copolymerization using a co-solvent mixture of cyclohexane and triethylamine, of varied relative compositions to probe the impact on compositional drift (statistical composition along the polymer chain). Copolymerization reactions are monitored online using in-situ Attenuated-Total-Reflectance Fourier Transform Infrared Spectroscopy (ATR-FTIR) to obtain monomer conversions as well as overall conversions in order to completely describe the copolymer compositional profiles. Compositional drift profiles are used to extract reactivity ratios using the Beckingham-Sanoja-Lynd approach to define the copolymer architecture and as a quantitative means of comparison. Conclusively, this system allows for the tuning of copolymer compositional profiles as desired with potential applications in designing polymer architectures with desired properties.

ACKNOWLEDGMENTS

It had, for unknown reasons, touched my heart as a child the first time my mom mentioned (and I saw it later, too) that she had thanked me in the acknowledgements section of her PhD dissertation for having been a cooperative baby (I was barely a year old when she finished). It would not be wrong to say that I've been looking forward excitedly to writing this section ever since I joined grad school at Auburn. Being the embodiment of my ardent gratitude for everyone who has been a vital part of my life as I sailed through my academic journey, this piece of writing is truly dear to me.

Firstly, I extend my heartfelt thanks to Dr. Bryan Beckingham who has stood by me throughout. To be very precise, he's undoubtedly the best advisor I ever could have asked for – an extremely supportive and a very compassionate human being. His passion for polymer science is evident in his answers to our questions and his expertise in the field is scintillating. Dr. Beckingham, you have played a supremely important part in shaping my graduate school experience so positively and transforming me for the good (probably unbeknownst to you), in a way I did not foresee. I cannot thank you enough!

I also would like to sincerely thank my committee members, Dr. Maria Auad and Dr. Andrew Adamczyk for all their support throughout. Dr Auad also happened to teach the course, "Structure and Properties of Polymers", at Auburn University two years ago and a lot of my work is related to the strong foundation she laid through her simple and holistic teaching.

I cannot even begin to imagine grad school without my lab peeps around! It was just Michael, Bree and me in my first semester in lab. You were and remain to be the first and the closest American friends I've had so far in Auburn; you guys are truly special. The fun we've

had, the jokes we've shared, the things you have taught, all the help you've given me over these years, the long academic and non-academic discussions, are all such invaluable memories! Thank you for being there for me, always. Luca, I cannot begin to thank you for all the patience you have had in staying with me in lab while I did most of my serious chemistry and I did get quite a lot of helpful Schlenk tips from you. Thank you! Vinita, we've had some interesting philosophical conversations at times and those meets over home-cooked food were so much fun! Thanks for being a smiling, reassuring presence in the group! Thanks to the Beckingham Polymer Research group's fun undergrads as well!

My greatest pillars of strength are my ever-encouraging parents (my husband joined this team of strength-givers since late 2017) who are both doctorate degree holders, simple, kind-hearted souls, always encouraging and letting their kids follow their hearts. I consider myself fortunate to have been born as their daughter. My little brother was this naughty and talkative kid when I left home to pursue my grad school but has slowly turned into a young man with a composed demeanor and of less words! Missed watching you grow into the present-Aashu but, you were always there saying, "You'll be fine, worry not!" like you were the elder one of us. Thanks a lot, Aashu. I surely cannot forget to thank my parents-in-law who became my parents as well. They saw my dream and instantly became a part of it, making me feel every bit like their own daughter! Thank you so much.

What would I do without friends? I truly have no idea. Some kept saying "We're always there for you" from India. The closest friends that I made after coming to Auburn University saw me through all my ups and downs, became my second family in a land far away from home. The memories I have with you guys are unforgettable and I shall always cherish them.

Vikram, the man of my dreams (and luckily, became my reality!), to you I say – your love, comforting words, positive attitude, innumerably hilarious jokes, amazing advice and constant support came into my life at the right time and kept me going. You became the peace and solace I had forever sought in life. After nearly a year of having stayed away from each other,

I now look forward with utmost glee, to a long, fun life with you! Please don't be mad and be just as nice as you've been so far if I ever say that I want to earn a PhD, next!

Finally, I would like to dedicate this Thesis to my grandfather whom I lost in December 2018. He was forever so encouraging of his grandchildren and always told us to follow our hearts relentlessly. His time-management skills, punctuality and discipline originating from his Army life has held me in good stead and will continue to do so. You are missed and your memories shall be cherished forever. A big salute to you, Captain G Krishnamurthy!

TABLE OF CONTENTS

LIST OF FIGURES

LIST OF TABLES

CHAPTER 1: INTRODUCTION AND BACKGROUND

1.1 Thesis Objective

This Thesis examines the synthesis and characterization of multicomponent polymer systems. Multi-component polymer systems are everywhere as blending or copolymerizing or arranging different polymer structures within a material allows for tremendous latitude in tuning material properties.[1–9] One primary variable in tuning properties in multicomponent polymer systems is the relative composition of the different polymers they are comprised of. Here, low-field ^{1}H NMR Spectroscopy (60 MHz), a newly commercially available technology, is examined as a low-cost alternative to expensive (in capital cost and maintenance cost) higher-field NMR spectrometers (> 250 MHz) for the compositional analysis of multicomponent polymer systems, namely polymer blends and block copolymers (Chapter 3)[10]. Results from a low-field spectrometer are directly compared to those from a high-field spectrometer and found to be quantitative within typically accepted variation from traditional high-field NMR spectroscopy.[10] Next, in Chapter 4, a co-solvent system (cyclohexane and triethylamine) of varied composition is utilized to vary the compositional drift (statistical composition along the polymer chain) in the copolymerization of styrene and isoprene. Copolymerization reactions are monitored with in situ Attenuated-Total-Reflectance Fourier Transform Infrared Spectroscopy (ATR-FTIR) to obtain monomer conversions to fully describe the statistical copolymer compositional profile. These profiles are utilized to extract reactivity ratios using the Beckingham-Sanoja-Lynd approach[11,12]. Overall, this system allows for tuning compositional profile as desired with potential applications in designing polymer architectures with desired properties.

1.2 Background

Polymer science has come a long way since its foundation was laid in the 1920s by Hermann Staudinger who went on to win the Nobel Prize for Chemistry in 1953. In 1908, Bakelite had become the first synthetically produced plastic and the World War II further caused a boom in the plastic industry due to the increased demand (both in quantity and properties) and scarcity of materials.[13] Polymeric materials have since become ubiquitous in our daily lives due to the breadth of material properties afforded by a variation in molecular architecture, chemical microstructure and functionality. There has been a continuous need to synthesize newer and better materials to cater to the ever-increasing applications as well as for finding improved substitutes for the existing applications which calls for a profound understanding of their chemistries, structures and the means to produce them.

So, what exactly is a polymer? Polymers can be broadly described as macromolecules consisting of long chains of repeating units called 'mers' linked together via covalent bonds. A special class of polymers of interest in this work are copolymers which are composed of more than one kind of mers or monomers. These materials are related to the traditional and industrially significant way of tuning bulk polymer properties for target applications through polymer blending which involves mixing two or more polymers to obtain distinct desired properties. Both these strategies for achieving materials of desired properties are multicomponent polymer systems, however copolymers incorporate these multiple polymer structures within the same molecule while blends mix (when possible) polymers of different structures.

In the analysis of multicomponent polymer systems, such as polymer blends and statistical copolymers, accurate characterization of the polymer blend or statistical copolymer composition is crucial. Typically, this analysis is performed using ^{1}H Nuclear Magnetic Resonance (NMR) Spectroscopy.[14–16,17] NMR spectroscopy utilizes the property of spin possessed by certain atomic nuclei, commonly ^{1}H and ^{13}C amongst many others (^{19}F, ^{17}O). When a sample is placed in an

external magnetic field, the randomly oriented nuclear spins tend to orient themselves either with the external field or against it.[18] The nuclei aligned with the magnetic field when subjected to electromagnetic radiation of a proper frequency, will absorb energy to align themselves against the field which is a higher energy state. When this spin-flip occurs, the nuclei are said to be in 'resonance' with the field.[18] The signal in NMR is produced by the absorption of electromagnetic radiation of the appropriate frequency which causes the spin-flip. ^{1}H NMR spectroscopy is particularly useful for determining polymer chemical structure and composition as nearly all polymers have abundant and distinct protons for analysis. Additionally, ^{1}H NMR spectroscopy yields quantitative chemical group concentrations without prior calibration. This has led ^{1}H NMR spectroscopy to become a routine method for the molecular characterization of polymers.

Over the last several decades NMR spectrometers have improved significantly, and current state-of-the-art spectrometers have increasingly high magnetic fields (i.e. Bruker Aeon 1 GHz Spectrometer). The increase in magnetic field strength has led to several orders of magnitude improvement in sensitivity.[19,20] High-field—where we denote high-field as > 5.8 T field strength (or alternatively > 250 MHz)—NMR spectrometers require cryogenic cooling due to their superconducting magnets and advanced probes as well as staffing by dedicated professionals due to the numerous, and at times very complex, NMR experiments that can be performed and the associated upkeep and maintenance requirements.[21] Unfortunately, due to the high capital and operating costs associated with high-field spectrometers, NMR spectroscopy is not commonly considered a low-cost analysis technique. However, the recent development of commercially available low-field benchtop NMR spectrometers may provide a less expensive alternative to higher field, and costlier, NMR spectrometers once validated for desired analyses.[22–24] Consequently, there has been an increased interest in the applying low-field NMR spectroscopy to polymer analysis and efforts have been made to benchmark and validate these instruments for various applications.[25–29] The benchmarking of a low-field NMR spectrometer (60 MHz) for the

compositional analysis of polymer blends, statistical copolymers and block copolymers is of particular interest and is the objective of Chapter 3 of this Thesis.

In contrast to polymer blending, simultaneous polymerization of multiple monomers is a strategy employed to synthesize polymers with varied properties by varying the comonomer compositions or controlling the distribution of monomers across the polymer chains.[30–36] The local and long range ordering of polymer materials has a profound impact on their properties. In general, the nature of a polymer chain's chemistry depends on how the monomers are incorporated during the polymerization and how the monomer incorporation can be manipulated to achieve desired polymer properties. There are numerous polymerization chemistries amenable to copolymerization (free-radical, cationic, RAFT, GRIM, etc.), however our focus is anionic copolymerization.

Anionic polymerization proceeds by the initiation of an unsaturated monomer through an organometallic species or compound.[37,38] Under specific conditions, anionic polymerizations can proceed without a termination step and the chain propagation continues until all the monomer is exhausted; the living chain end however, will again propagate if an additional quantity of monomer is added. This type of polymerization has been termed as 'living polymerization'.[39] Alkyllithium initiators have been used most extensively to carry out anionic living polymerizations due to their solubility in hydrocarbon solvents[40] and we make use of these initiators in the presented work, as well. Initiation can take place either through nucleophilic addition or electron transfer.[38,41,42] The nucleophilic initiation reaction scheme specific to the anionic living polymerizations in this thesis using sec-Butyllithium has been presented in Figure 1.1.

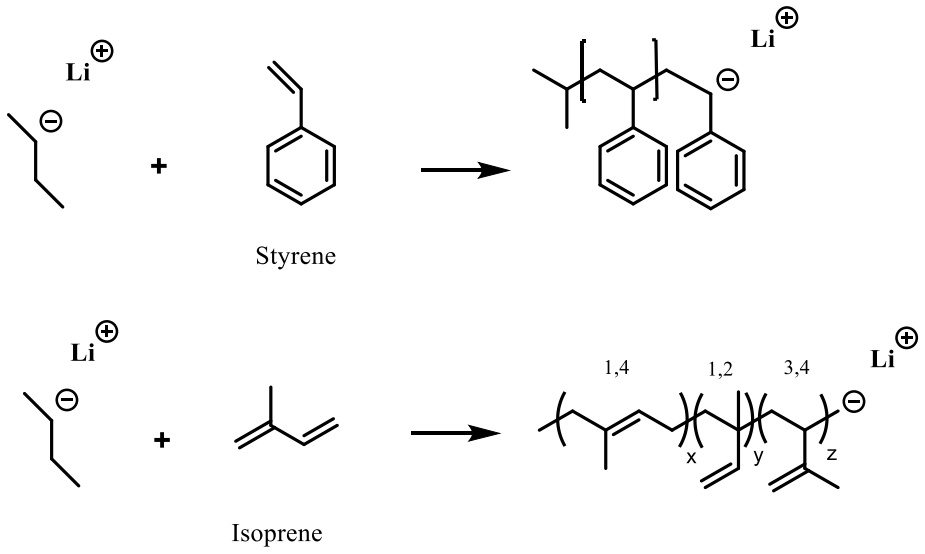

Figure 1.1 Initiation of styrene and isoprene monomers using sec-Butyllithium initiator.

Anionic living copolymerization is sensitive to changes in polymerization environment and hence this method is well suited for synthesizing copolymers with control over the polymer architecture by manipulating the propagation steps.[38] Compositional control in anionic living chain copolymerization is tied to the intrinsic reactivity (or relative reactivity) of the two monomers. This relative reactivity is typically described with a terminal model of copolymerization kinetics and the reactivity ratios, for instance r_S and r_I for the copolymerization of styrene and isoprene, describe the tendency of a propagating chain end species to self-propagate and enchain its own type of monomer over that of the other monomer. In this way, reactivity ratios represent the compositional drift that results from the difference in monomer reactivity during the copolymerization and have been a common metric for classifying or discerning between the four well-established types of copolymerizations - gradient, blocky, alternating and random (see Figure 1.1).[14,15,30,42–44]

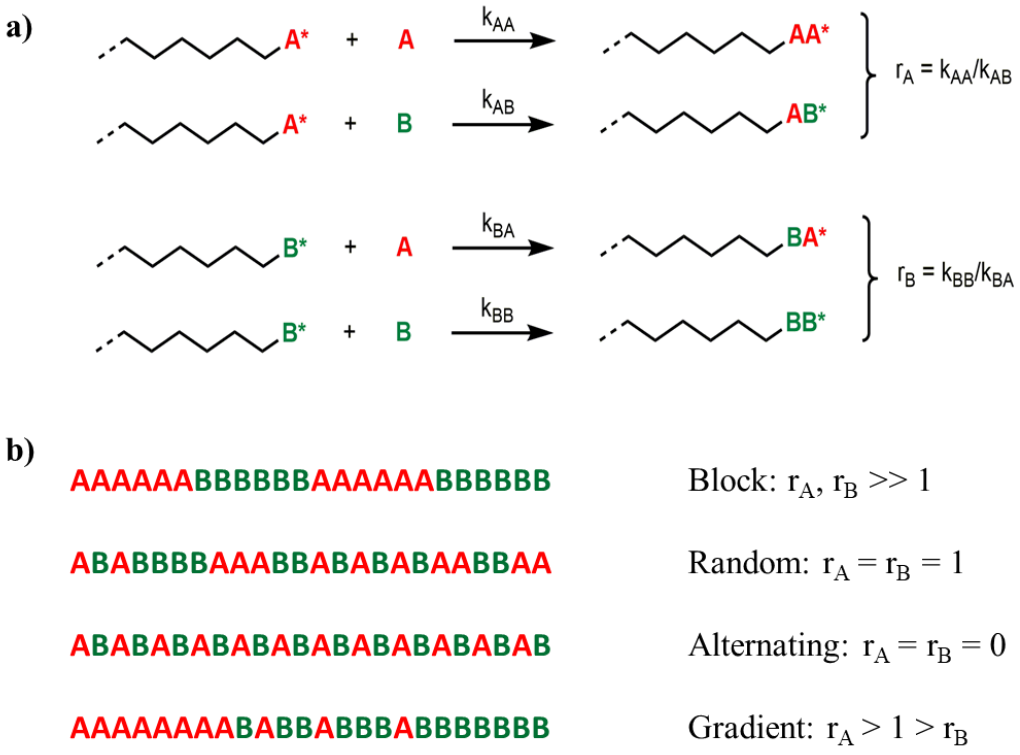

Figure 1.2 The most common types of copolymerizations in relation to the reactivity ratios

Reactivity ratios are distinct for pairs of monomers under specific reaction conditions. They are temperature and solvent dependent and may be influenced by the presence of additives. As an example, alkyllithium-initiated copolymerizations of styrene and butadiene (SB) in cyclohexane yields a strong gradient copolymer (almost a pure block copolymer) where butadiene is preferentially added in the initial stages of copolymerization and a significant fraction of styrene monomer begins to add onto the chain only once nearly all of the butadiene has been exhausted. Alternatively, the opposite structure is obtained (styrene preferred at initial times) when the copolymerization is performed in tetrahydrofuran. A lot of research work has been carried out with various solvents giving rise to a varied spectrum of monomer incorporation distributions.[45–47] Of significant importance to the work that has been presented in Chapter 4 of this thesis are the findings of Kelley and Tobolsky's work[48], where it was shown that triethylamine (TEA) generateed nearly-flat compositional profiles for styrene/isoprene (SI) copolymerizations. This was studied further by Beckingham and Register and they concluded that usage of 50/50 (v/v) Cyclohexane/Triethylamine

mixture resulted in the copolymerization of styrene and isoprene with no down-chain compositional gradient.[32] Here, this prior work is extended to examine how the gradient structure can be varied by carefully tuning the cosolvent polymerization environment.

Copolymerizations have been monitored in various ways[49] such as the offline method of the classical aliquot-collection and subsequent analysis[32], as well online monitoring via NMR Spectroscopy[50–52], IR spectroscopy[53] and other such techniques.[49] In this thesis, the compositional drift is attempted to be controlled by carrying out copolymerizations of styrene and isoprene in solvent mixtures of distinct volumetric ratios of cyclohexane (CH) and triethylamine (TEA), varying between 100/0 CH/TEA and 50/50 CH/TEA. Here, we monitor these copolymerization reactions using custom-built glass reactors outfitted for performing in-situ ATR-FTIR Spectroscopy. Higher TEA contents were not used in the solvent as polystyrene homopolymer is insoluble in pure TEA and as the primary goal was controlling compositional drift between the extrema of a block copolymer-like architecture and a random copolymer architecture which can be achieved within the limits examined.

1.3 Thesis Organization

Chapter 1.1 outlined the objectives of this work carried and an overview of the polymer materials and synthesis techniques involved in its realization. Chapter 1.2 provided additional background on polymers, copolymers, polymer synthesis and characterization important to this work. In Chapter 2, the general experimental procedures used in the work are presented. Chapter 3 examines the use of low-field ^{1}H NMR spectroscopy as a promising tool for the routine characterization of multicomponent polymer systems including polymer blends and copolymers, while drawing comparison with high-field strength ^{1}H NMR spectroscopy (as published in *RSC Analyst*). Chapter 4 explores tuning the compositional drift in styrene/isoprene (SI) copolymerization by varying the solvent environment, i.e. using different volumetric ratios of cyclohexane/triethylamine and analyzing the effects that triethylamine content has on the

copolymerization reactivity ratios. Lastly, Chapter 5 presents a consolidation of all the conclusive results and the scope for future research that this thesis instigates.

1.4 References

(1) Singh, K.; Blümich, B. *Polymer (Guildf)*. **2018**, *141*, 154–165.

(2) Beckingham, B. S.; Register, R. A. *Macromolecules* **2013**, *46* (8), 3084–3091.

(3) Beckingham, B. S.; Burns, A. B.; Register, R. A. *Macromolecules* **2013**, *46* (7), 2760–2766.

(4) Kuan, W.-F.; Remy, R.; Mackay, M. E.; Epps, T. H. **2015**.

(5) Patterson, A. L.; Danielsen, S. P. O.; Yu, B.; Davidson, E. C.; Fredrickson, G. H.; Segalman, R. A. *Macromolecules* **2019**, *52* (3), 1277–1286.

(6) Tsai, S. D.; Register, R. A. *Macromol. Chem. Phys.* **2018**, *219* (11), 1–7.

(7) Faghihi, F.; Hazendonk, P. *Polymer (Guildf)*. **2017**, *128*, 31–39.

(8) Trigg, E. B.; Tiegs, B. J.; Coates, G. W.; Winey, K. I. **2019**.

(9) Aplan, M. P.; Gomez, E. D. **2017**.

(10) Chakrapani, S. B.; Minkler, M. J.; Beckingham, B. S. *Analyst* **2019**, *144* (5), 1679–1686.

(11) Beckingham, B. S.; Sanoja, G. E.; Lynd, N. A. *Macromolecules* **2015**, *48* (19), 6922–6930.

(12) Lynd, N. A.; Ferrier, R. C.; Beckingham, B. S. *Macromolecules* **2019**, *52*, 2277–2285.

(13) Hermann Staudinger Foundation of Polymer Science - Landmark - American Chemical Society https://www.acs.org/content/acs/en/education/whatischemistry/landmarks/staudingerpolymerscience.html (accessed Feb 16, 2019).

(14) Barlow, J. W.; Paul, D. R. *Polym. Eng. Sci.* **1981**, *21* (15), 985–996.

(15) L. A. Utracki; C. Wilkie. *Polymer Blends Handbook*; Springer, 2014.

(16) Fryling, C. F. High Impact Polystyrene. 3,144,420, 1964.

(17) Rozentsvet, V. A.; Khachaturov, A. S.; Ivanova, V. P. *Polym. Sci.* **2009**, *51* (8), 870–876.

(18) Pavia, D. L.; Lampman, G. M.; Kriz, G. S. *Introduction to Spectroscopy*, 3rd ed.; Brooks/Cole-Thomson Learning, 2001.

(19) Gilbert, D. G.; Donald, A. M. *Toughening mechanisms in high impact polystyrene*; 1986; Vol. 21.

(20) Hobbs, S. Y. *Polym. Eng. Sci.* **1986**, *26* (1), 74–81.

(21) Hay, A. S. *J. Polym. Sci. Part A Polym. Chem.* **1998**, *36*, 505–517.

(22) Tanaka, Y.; Takeuchi, Y.; Kobayashi, M.; Tadokoro, H. *J. Polym. Sci. Part A-2 Polym. Phys.* **1971**, *9* (1), 43–57.

(23) Stuart, B. *Polymer Analysis*; Wiley, 2008; Vol. 9783527336.

(24) Santee, E. R.; Chang, R.; Morton, M. *300 MHz proton NMR of polybutadiene: Measurement of cis-trans isomeric content*; 1973; Vol. 11.

(25) Kovacs, H.; Moskau, D.; Spraul, M. *Prog. Nucl. Magn. Reson. Spectrosc.* **2005**, *46* (2–3), 131–155.

(26) H. Gunther. *NMR Spectroscopy: BAsic Principles, Concepts and Applications in Chemistry*; Wiley, 1995.

(27) Spiess, H. W. *Macromolecules* **2017**, *50*, 1761–1777.

(28) Blümich, B. *TrAC - Trends Anal. Chem.* **2016**, *83*, 2–11.

(29) Adams, A. *Trends Anal. Chem.* **2016**, *83*, 107–119.

(30) Wu, S. *Polymer (Guildf).* **1985**, *26*, 1855–1863.

(31) Kuan, W.-F.; Roy, R.; Rong, L.; Hsiao, B. S.; Epps, T. H. *ACS Macro Lett.* **2012**, *1* (4), 519–523.

(32) Beckingham, B. S.; Register, R. A. *Macromolecules* **2011**, *44* (11), 4313–4319.

(33) Obermeier, B.; Frey, H. *Bioconjug. Chem.* **2011**, *22* (3), 436–444.

(34) Zhang, W.; Allgaier, J.; Zorn, R.; Willbold, S. *Macromolecules* **2013**, *46* (10), 3931–3938.

(35) Beckingham, B. S.; Burns, A. B.; Register, R. A. *Macromolecules* **2013**, *46* (7), 2760–2766.

(36) Bergman, J. A.; Cochran, E. W.; Heinen, J. M. *Polymer (Guildf).* **2014**, *55*, 4206–4215.

(37) Morton, M. *Ind. Eng. Chem. Prod. Res. Dev.* **1972**, *11* (1), 106.

(38) Morton, M. *Anionic Polymerization: Principles and Practice*; Academic Press: New York, 1983.

(39) Szwarc, M. *Nature* **1956**, *178*, 1168–1169.

(40) Young, R. J.; Lovell, P. A. *Introduction to Polymers*, 2nd ed.; Cheltenham, United Kingdom: Stanley Thornes Ltd., 1991.

(41) Stevens, M. A. *Polymer Chemistry: An Introduction*; New York: Oxford University Press, 1999.

(42) Odian, G. *Principles of Polymerization*, 4th ed.; John Wiley & Sons, Inc., New York, 2004.

(43) Krishnamoorti, R.; Graessley, W. W.; Dee, G. T.; Walsh, D. J.; Fetters, L. J.; Lohse, D. J. *Macromolecules* **1996**, *29*, 367–376.

(44) Coleman, M. M.; Painter, P. C. *Progress in Polymer Science*. 1995, pp 1–59.

(45) Antkowiak, T. A.; Obesrster, A. E.; A. F. Halasa. *J. Polym. Sci. Part A Polym. Chem.* **1972**, *10*, 1319–1334.

(46) Annigh6fer, F.; Gronski, W. *Colloid Polym. Sci.* **1983**, *261* (1), 15–25.

(47) Chang, C. C.; Halasa, A. F.; Miller Jr, J. W.; Hsu, W. L. *Polym. Int.* **1994**, *33*, 151–159.

(48) Kelley, D. J.; Tobolsky, A. V. *Am. Chem. Soc.* **1959**, *81*, 1597–1600.

(49) Haven, J. J.; Junkers, T. *European J. Org. Chem.* **2017**, *2017* (44), 6474–6482.

(50) Dalitz, F.; Cudaj, M.; Maiwald, M.; Guthausen, G. *Prog. Nucl. Magn. Reson. Spectrosc.* **2012**, *60*, 52–70.

(51) Natalello, A.; Werre, M.; Alkan, A.; Frey, H. *Macromolecules* **2013**, *46* (21), 8467–8471.

(52) Elipe, M. V. S.; Milburn, R. R. *Magn. Reson. Chem.* **2016**, *54* (6), 437–443.

(53) Quinebèche, S.; Navarro, C.; Gnanou, Y.; Fontanille, M. *Polymer (Guildf).* **2009**, *50*, 1351–1357.

CHAPTER 2: EXPERIMENTAL METHODS

This chapter provides general information about the various techniques used in the realization of this work. Additional, specific details on the experimental and synthetic procedures used will be presented in the experimental sections of the relevant chapters. Anecdotes on general procedures to synthesize the various homopolymers and copolymers utilizing in-situ attenuated-total-reflectance Fourier Transform Infrared (ATR-FTIR) spectroscopy reaction monitoring and their post-synthesis characterization by using ^{1}H NMR spectroscopy, gel permeation chromatography (GPC) and Differential scanning calorimetry (DSC) are provided here.

2.1 Anionic Polymerization and Copolymerization

Anionic initiators are highly susceptible to termination by oxygen or moisture requiring additional care be taken in the preparation of solvents, monomers and glassware that will be utilized for carrying out the polymerizations. Purification of solvents and monomers were performed on a dual manifold Schlenk line that allows for access to both nitrogen and vacuum of 0 - 40 mtorr created by Edwards RV3 mechanical pump and a liquid nitrogen trap. Glove box by Vacuum Technology Inc (<0.1 ppm O_2, <0.1 ppm H_2O) using Nitrogen as the working gas is employed for transfer of initiators and to carry out polymerizations within as and when necessary. All glassware used were washed and oven-dried prior to usage.

Initiators – n-butyllithium (2.2 M in hexane) from Alfa Aesar, di-n-butylmagnesium (1.0 M in heptane), sec-butyllithium (1.4 M in cyclohexane) and tert-butyllithium (1.7 M in pentane) from Aldrich Chemical Company were used as received. *Caution! tert-butyllithium is a pyrophoric and moisture-sensitive material and should be handled with appropriate care.* Styrene monomer

(Aldrich) was dried over di-n-butylmagnesium, degassed by carrying out a sufficient number of freeze-pump-thaw (FPT) cycles and vacuum distilled prior to use. In a like manner, isoprene monomer (Aldrich) was dried over n-butyllithium, degassed by FPT cycles, and vacuum distilled prior to use. Cyclohexane and triethylamine (used as the solvents for the anionic polymerizations) were stirred over diphenylhexyllithium (an adduct of sec-butyllithium and 1,1 diphenylethylene), freeze-pump-thawed and vacuum distilled prior to use. Methanol used for terminating the polymerizations was degassed via FPT cycles before usage. All polymers and copolymers were synthesized in 100 mL of solvent consisting of varying volumetric ratios of cyclohexane and triethylamine for different polymers, unless otherwise mentioned. 10 g of polymer was set to be the desired copolymer target weight. All copolymerizations were monitored using a Mettler Toledo ReactIR15 attenuated-total-reflectance Fourier Transform Infrared (ATR-FTIR) spectroscopy probe system (see Figure 2.1) and were carried out at ~40 °C.

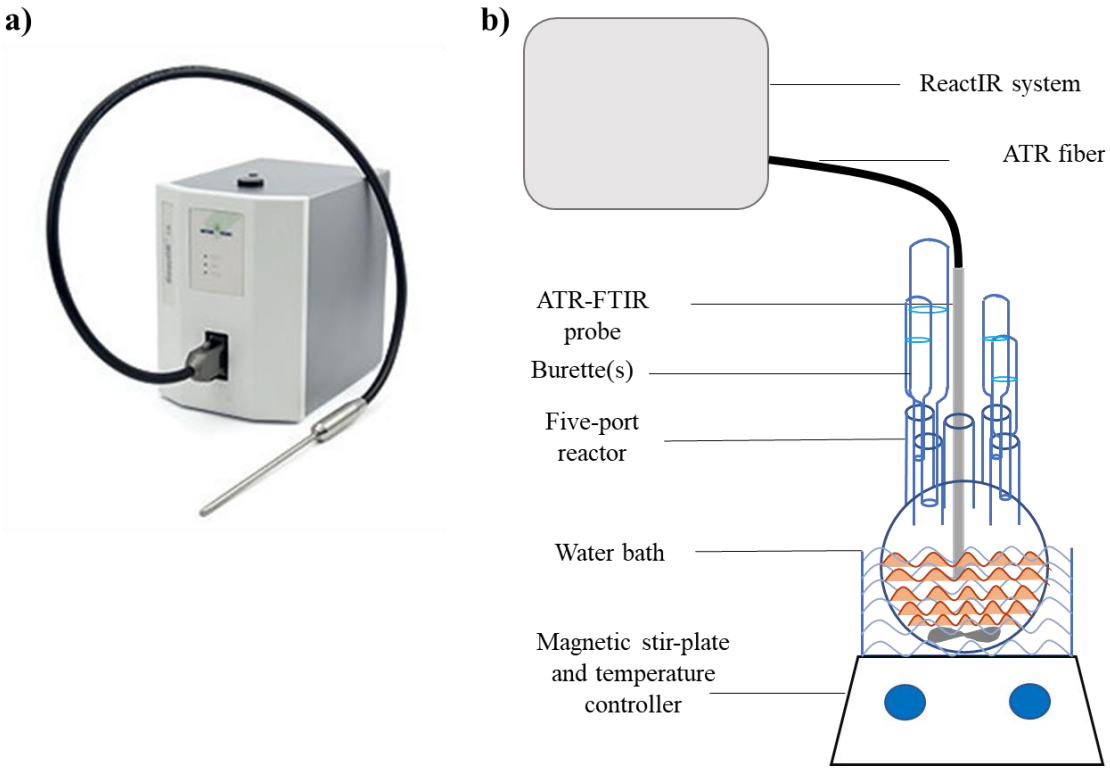

Figure 2.1 a) Mettler Toledo's ReactIR 15 system b) A highly simplified schematic figure of the setup used for ATR-FTIR-monitored-copolymerizations.

To carry out in-situ ATR FTIR spectroscopy monitored anionic copolymerizations, required quantities of cleaned solvents, cleaned monomers and initiator, sec- Butyllithium (with 5 mL of Cyclohexane) were syringe transferred into three separate air-tight glass burettes within a glovebox. A custom-built five-port glass reactor with the ATR-FTIR spectroscopy probe inserted, was purged with nitrogen gas through a custom adapter connected to the nitrogen manifold of the Schlenk line. The reactor was maintained at the desired temperature (40 °C) using a water bath. The three burettes were fitted onto the reactor as the nitrogen flow was decreased. The reactor was then evacuated by connecting to the vacuum manifold of the Schlenk line to ~150 mtorr before sealing from the Schlenk line and commencing the FTIR spectral acquisition at one-minute time intervals. Solvent, monomer and then initiator were charged into the reactor, with the ATR FTIR spectroscopy probe acquiring a spectrum at 1-minute intervals and at least 5 scans were acquired between subsequent additions to ensure stable spectra for solvent subtraction. The polymerization was then monitored by tracking characteristic styrene and isoprene peaks—that are not present in the polymer—on the acquired spectra in order to ensure complete conversion of monomer before termination. Once complete, the polymerization was terminated by injecting an adequate quantity of degassed methanol into the reactor through a septum located on the custom Schlenk adapter. A sample of the final reaction mixture was immediately transferred to an NMR tube and analyzed using an Oxford Instruments Pulsar 60 MHz ^{1}H NMR spectrometer to extract solvent composition and the final polystyrene and polyisoprene content of the copolymers.

The copolymers are named as shown in Table 2.1; ‘SI’ as they are composed of styrene and isoprene, the first number represents the volume percent of TEA in the solvent and the second number is the mole percent polystyrene in the copolymer. For example, SI-0/29 was synthesized in pure cyclohexane (0 % triethylamine) and contains 29 mol % polystyrene.

Table 2.1 A table of copolymers synthesized, their initiation temperatures and the volume of triethylamine (TEA) used in the solvent.

Polymer	Temperature of Initiation (^{o}C)	Volume %TEA	Mol % Styrene
SI-0/29	39	0	29
SI-9/28	39	9	28
SI-28/31	41	28	31
SI-29/26	43	29	26
SI-40/31	40	40	31
SI-41/31	38	41	31
SI-50/26	40	50	26

2.2 Polymer Characterization Techniques

This section describes the various techniques used to characterize molecular weight, composition and physical properties of the polymers synthesized and studied in this work.

2.2.1 Proton Nuclear Magnetic Resonance Spectroscopy

Proton Nuclear Magnetic Resonance (^{1}H NMR) Spectroscopy was used to determine the compositions of polymers and solvents systems involved in this work. An Oxford Instruments Pulsar 60 MHz spectrometer (low-field) and a Bruker Avance 400 MHz spectrometer (high-field) were the instruments used in this work. In Chapter 3, the capability of the 60 MHz spectrometer is compared to the 400 MHz spectrometer for the quantitative determination of the composition of block copolymers and polymer blends. Generally, polymer samples were prepared by dissolving the polymer at a concentration of about 10 mg/mL in deuterated chloroform and doped with a few drops of tetramethylsilane (TMS). Final copolymerization reaction mixtures after termination, were analyzed neat and doped with a few drops of TMS on the 60 MHz spectrometer in order to accurately position the spectra in ppm space. Note that the 60 MHz ^{1}H NMR instrument used does not require deuterated solvents in order to obtain spectral stability unlike in case of the high-field instruments. Copolymerization-related NMR spectra were all acquired with 256 scans and a recycle delay of 10 seconds. The spectra were baselined, phase corrected, and the TMS peak

was set as the reference to 0.00 ppm. Relevant peak assignments for the various polystyrene, polyisoprene and poly(methyl methacrylate) protons are shown in Table 2.2, while the peak assignments for cyclohexane and triethylamine are shown in Table 2.3.[1] The overall copolymer composition, solvent composition as well as the microstructural composition of isoprene can be determined based on these peak assignments and the number of contributing protons. The triethylamine peak at 2.53 ppm was used for determining the solvent composition.

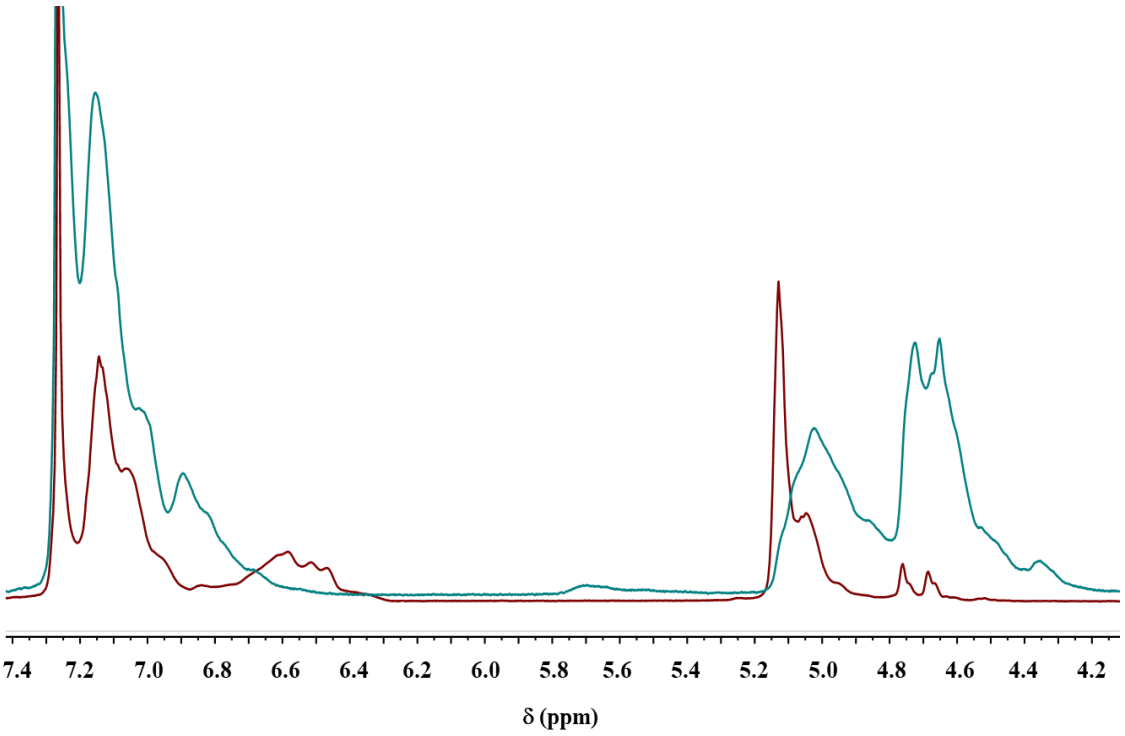

Figure 2.2 400 MHz ^{1}H NMR spectra superimposed – SI-0/29, synthesized in neat cyclohexane (red) and SI-50/26, synthesized in 50/50 v/v mixture of TEA/CH (blue).

Table 2.2 ^{1}H NMR Peak Assignments for Polyisoprene, Polystyrene and Poly(methyl methacrylate)[2–5]

Polymer	Protons	δ (ppm)
Polystyrene	meta- and para- =C**H**	7.1
	ortho- =C**H**	6.8
Polyisoprene	1,4 =C**H**-	5.1
	3,4 =C**H$_2$**	4.8
	1,2 =C**H$_2$**	4.9
	1,2 -C**H**=	5.7
Poly (methyl methacrylate)	Ester methyl -C**H$_3$**	3.6

Table 2.3 ^{1}H NMR Peak Assignments for Cyclohexane and Triethylamine in $CDCl_3$[1]

Solvent	Protons	δ (ppm)
Cyclohexane	-C**H$_2$**	1.43
Triethylamine	-C**H$_3$**	1.03
	-C**H$_2$**	2.53

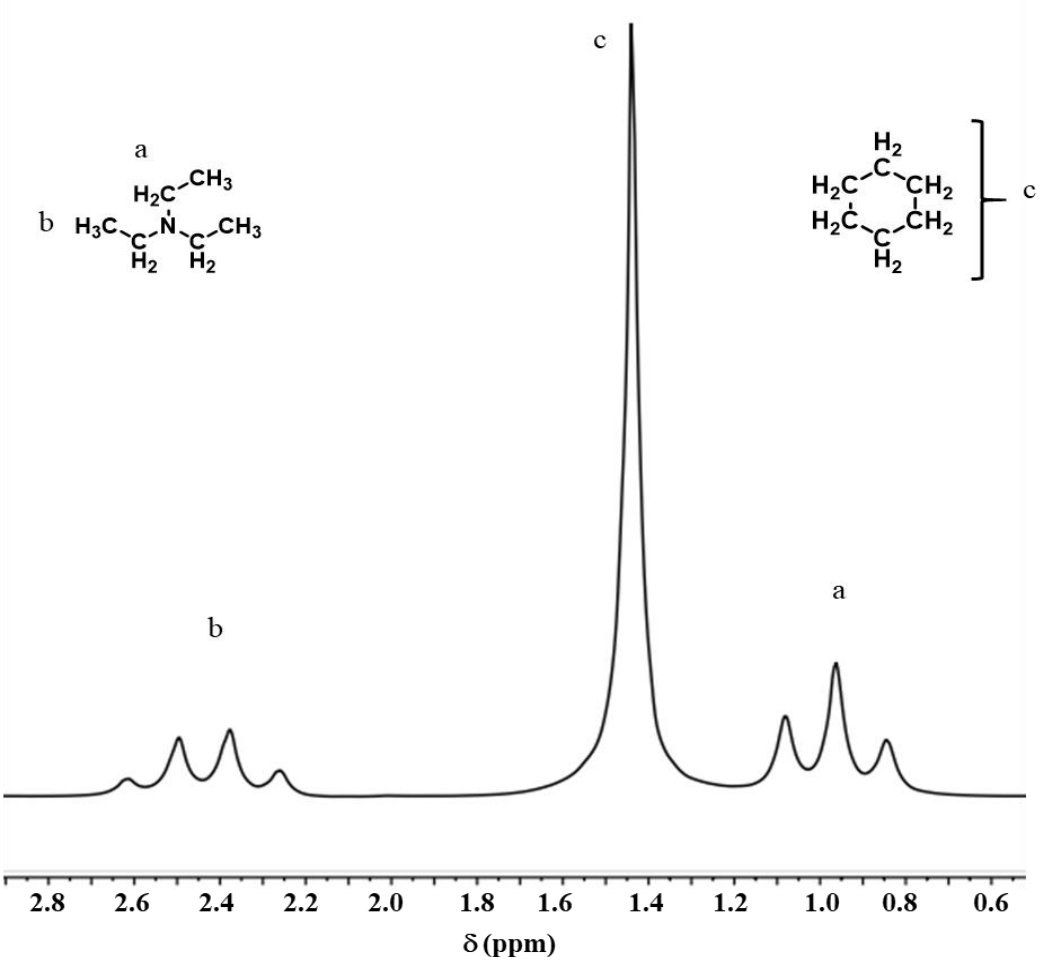

Figure 2.3 Triethylamine and Cyclohexane ^{1}H NMR peaks acquired using a 60 MHz NMR spectrometer.

2.2.2 Differential Scanning Calorimetry (DSC)

Differential Scanning Calorimetry (DSC) was used to ascertain the glass transition temperatures of all the synthesized polymers and copolymers. In amorphous materials, the glass transition temperature[6] denotes a reversible transition in material behavior. Below the glass transition temperature (T_g), polymers are glassy (hard and relatively brittle), while above the T_g polymers are viscous fluids or rubbery solids. T_g marks the onset of coordinated motions of polymer chains enabling the polymers to flow as the temperature is increased.[6]

Approximately 5-10 mg of the polymer sample is weighed out into an aluminum pan from TA Instruments, crimped and placed on one furnace while an identical, empty reference pan is

placed on the other. When the temperature of the two pans are increased or decreased at a programmed rate, the differential heat flow required to maintain both the pans at the same temperature is measured by the instrument. A Q20 DSC and its cooler by Refrigerated Cooling System 90, both obtained from TA Instruments were used for acquiring the data in this work.

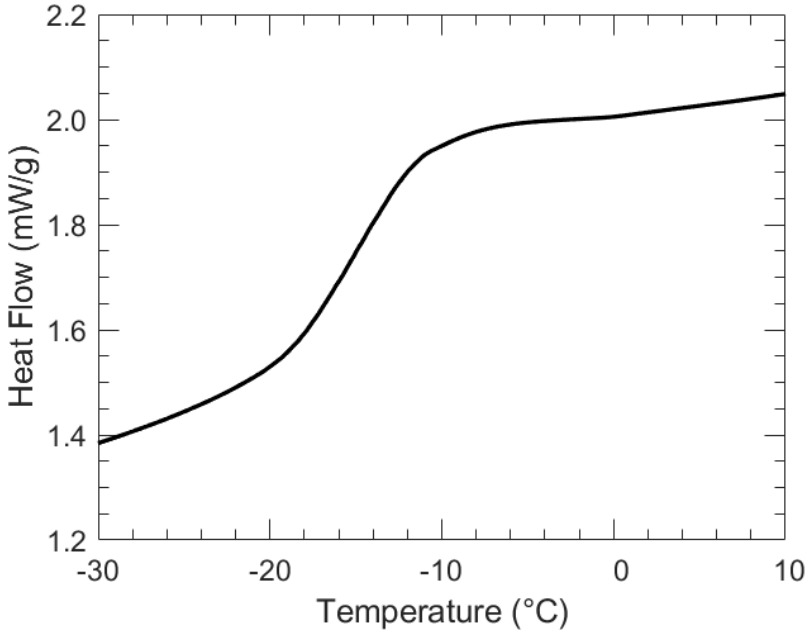

Figure 2.4 DSC plot of SI-28/31 showing a T_g of -15 °C

2.2.3 Gel Permeation Chromatography (GPC)

Gel permeation chromatography (GPC) was used in the determination of molecular weight and dispersity of all the polymers and copolymers. GPC is a type of size exclusion chromatography which is typically used for higher molecular weight substances such as polymers and yields information on the molecular sizes of the molecules in the sample and consequently the distribution of molecular sizes as characterized by the dispersity.

The number average molecular weight, M_n is the statistical average molecular weight of all the polymer chains in the sample and is defined as:

$$M_n = \frac{\sum N_i M_i}{\sum N_i} \quad (2.\ 1)$$

where, M_i is the molecular weight of a chain and N_i is the number of chains of that molecular weight. If M_n is quoted for a molecular weight distribution, it means that there are equal numbers of molecules on either side of M_n in the distribution. M_n is the molecular weight used when designing the polymerization target as it is directly related to the average number of repeat units in the synthesized polymer. The weight average molecular weight is defined as:

$$M_w = \frac{\sum N_i M_i^2}{\sum N_i M_i} \quad (2.\ 2)$$

As opposed to M_n, M_w takes the molecular weights of a chain into account in determining its contribution to the molecular weight average. The more massive a polymer chain in the sample, the greater its contribution to the M_w. M_w is determined by methods that are sensitive to the molecular size, such as light scattering techniques. When M_w is quoted for a molecular weight distribution, there is an equal weight of molecules on either side of M_w in the distribution. Dispersity (*Đ*) formerly known as polydispersity index (PDI), is a measure of the broadness of a molecular weight distribution of a polymer and is defined as:

$$Đ = \frac{M_w}{M_n} \quad (2.\ 3)$$

The larger the *Đ*, broader is the molecular weight distribution. A monodisperse polymer in which all the chain lengths are equal has an $M_w/M_n = 1$. The best controlled synthetic polymers (narrow polymers used for calibrations) have *Đ* = 1.02 to 1.10. Step polymerization reactions usually yield values of *Đ* of ~ 2.0. Anionic polymerization, of interest here, is used for the synthesis of narrow

molecular weight distribution polymers due to the tight control over initiation, propagation and termination.

All the polymer samples analyzed here were prepared at 1 mg/mL in HPLC grade tetrahydrofuran (THF) that was stabilized with ~300 ppm butylated hydroxytoluene (BHT). The polymers were left to dissolve in THF overnight and the polymer solutions are passed through 0.2 μm nylon filters into a 2 mL vials from Malvern Panalytical (Malvern, UK) which are then placed in the GPC's autosampler. The system used to conduct the presented work is a Malvern OmniSEC Resolve and Reveal system that includes a refractometer, viscometer, ultraviolet/visible (UV/Vis) spectrophotometer, and dual angle light scattering. Two PL Gel Mixed-C columns with 5 μm pore size were used for this study and the mobile phase used is the above-mentioned THF. Conventional calibration method was used to calculate the Polystyrene-equivalent molecular weights of all the samples. The conventional method of calibration is carried out for the Refractive Index (RI) detector and relies on a series of nine known molecular weight polystyrene samples to generate a calibration curve. Figure 2.5 shows a typical GPC plot for one of the synthesized copolymers.

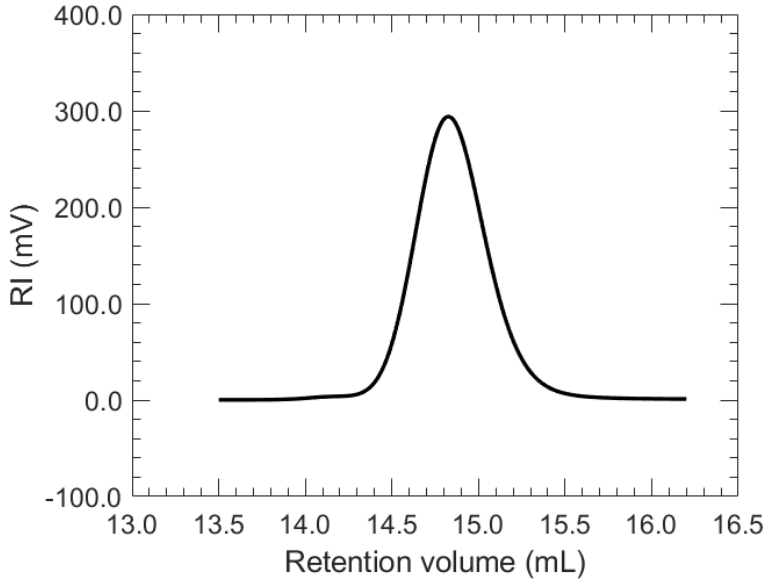

Figure 2.5 GPC plot of SI-9/28 showing a plot of the RI signal used to calculate the Polystyrene-equivalent molecular weight using the conventional calibration method. Mn = 6.7 kg/mol, and $Đ$ = 1.07.

2.3 References

(1) Fulmer, G. R.; Miller, A. J. M.; Sherden, N. H.; Gottlieb, H. E.; Nudelman, A.; Stoltz, B. M.; Bercaw, J. E.; Goldberg, K. I. *Organometallics* **2010**, *29*, 2176–2179.

(2) Tanaka, Y.; Takeuchi, Y.; Kobayashi, M.; Tadokoro, H. *J. Polym. Sci. Part A-2 Polym. Phys.* **1971**, *9* (1), 43–57.

(3) Santee, E. R.; Chang, R.; Morton, M. *300 MHz proton NMR of polybutadiene: Measurement of cis-trans isomeric content*; 1973; Vol. 11.

(4) Nagai, M.; Nishioka, A. *J. Polym. Sci. Part A-1 Polym. Chem.* **1968**, *6* (6), 1655–1660.

(5) Chakrapani, S. B.; Minkler, M. J.; Beckingham, B. S. *Analyst* **2019**, *144*.

(6) Sperling, L. H. *Introduction to Physical Polymer Science*, Fourth.; John Wiley & Sons, Inc., 2006.

CHAPTER 3: LOW-FIELD ^{1}H-NMR SPECTROSCOPY FOR COMPOSITIONAL ANALYSIS OF MULTICOMPONENT POLYMER SYSTEMS

3.1 Introduction

A classic and industrially important method for tuning material properties for target applications using polymeric materials is by mixing two chemically dissimilar polymers forming a polymer blend.[1–5] In the analysis of multicomponent polymer systems, such as polymer blends and statistical copolymers, the composition of the polymer blend and individual polymer chains is crucial. Typically, the composition of multicomponent polymer systems is characterized with ^{1}H Nuclear Magnetic Resonance (NMR) Spectroscopy.[6–8] ^{1}H NMR spectroscopy is particularly useful for determining polymer chemical structure and composition as nearly all polymers have abundant and distinct protons for analysis. Additionally, ^{1}H NMR spectroscopy yields quantitative chemical group concentrations without prior calibration. This has led ^{1}H NMR spectroscopy to become a routine method for the molecular characterization of polymers.

Over the last several decades NMR spectrometers have improved significantly, and current state-of-the-art spectrometers have increasingly high magnetic fields (i.e. Bruker Aeon 1 GHz Spectrometer).[9] It is currently common practice to refer to these high-field magnets by their corresponding magnetic field strength for hydrogen.

Equations 1 and 2 show the relationship between gyromagnetic ratio (γ_n) and spectrometer field strength (B_0):

$$\frac{\gamma_n}{2\pi} = \frac{\mu_N g_n}{h} \qquad (3.1)$$

$$f = \frac{\gamma_n}{2\pi} B_0 \qquad (3.2)$$

where, μ_N is the nuclear magneton, g_n is the g-factor for a nucleus, h is the Planck's constant and f is the frequency (MHz). To determine the frequency of a particular NMR spectrometer, the user to only multiply the field strength of the magnet (in Tesla) by $\gamma_n/2\pi$ or 42.577 Mhz T^{-1} for hydrogen (i.e., 1 GHz spectrometer has a field strength of 23.5 T).[10] The increase in magnetic field strength has led to several orders of magnitude improvement in sensitivity.[9,11] This increase in sensitivity is typically characterized as a signal to noise ratio which is proportional to both field strength and the number of scans acquired (n), as shown in Equation 3.

$$\frac{Signal}{Noise} \alpha B_0^{\frac{3}{2}} \sqrt{n} \qquad (3.2)$$

Thus, spectrometers with higher field strengths require less sample and will produce spectra with significantly sharper peaks.[10] High-field—where here we denote high-field as > 5.8 T field strength (or alternatively > 250 MHz)—NMR spectrometers require cryogenic cooling due to their superconducting magnets and advanced probes as well as staffing by dedicated professionals due to the numerous, and at times very complex, NMR experiments that can be performed and the associated upkeep and maintenance requirements.[8] Unfortunately, due to the high capital and operating costs associated with high-field spectrometers, NMR spectroscopy is not commonly considered a low-cost analysis technique. This is especially true for routine materials verification

such as quality control in industrial settings that commonly lack on-site advanced instrumentation facilities.

The recent development of commercially available low-field benchtop NMR spectrometers may provide a less expensive alternative to higher field, and costlier, NMR spectrometers once validated for desired analyses.[12–14] These low-field NMR spectrometers or compact "benchtop" NMR spectrometers feature permanent magnets with typical magnetic field strengths of 20-80 MHz (0.46-1.88 T), a lower capital cost, little to no operating expense, and have a small physical footprint. As a consequence of the lower field strength these spectrometers have lower overall sensitivity and spectral dispersion.[9,11,15] For the analysis of polymers, where peaks are characteristically broader than small molecule analogues, the lower spectral dispersion exacerbates issues with resonance overlap.[15] This resonance overlap can impede quantitative analysis of polymer materials with closely situated peak signatures using 1D ^{1}H NMR spectra much more at low-field than at high-field. Figure 3.1a shows spectra acquired with a 60 MHz benchtop spectrometer, a 250 MHz spectrometer, and a 400 MHz spectrometer. The spectra are reasonably similar; however, the spectra produced by higher field strength spectrometers appear cleaner with less visible noise. It should be noted that all three spectra were produced with 16 scans, standard acquisition parameters, and the data produced were processed in the same manner using MNOVA. The difference in the data is due to the frequencies at which protons are detected in each of the spectrometers. These differences can also be visualized by plotting the data in frequency space as shown in Figure 3.1b. This illustrates how at the expanded frequency space at higher field strength leads to improved resolution upon transformation into the same range of ppm space; i.e., the weaker the magnet, the narrower the spectrum in frequency space.

The above-mentioned issues with spectra quality notwithstanding, due to a recent surge in commercial availability of these instruments there has been increased interest in the application of low-field NMR spectroscopy and efforts have been made to benchmark and validate these

instruments for applications both old and new.[15–19] For instance, low-field spectrometers have recently been applied to quality control aspects of agricultural products (beef authenticity, oil adulteration, alcohol content, etc.).[19–22] For characterizing synthetic polymer materials, low-field NMR spectrometers have been applied to a variety of applications including monitoring polymerization kinetics, crystallization kinetics and crystallite/amorphous morphology, miscibility and dynamics, network crosslink density and swelling, composition and glass transition.[13,15,16,22–27] Low-field ^{1}H NMR spectroscopy has also been coupled with gel permeation chromatography for chemical identity mapping to molecular weight distributions.[28–30]

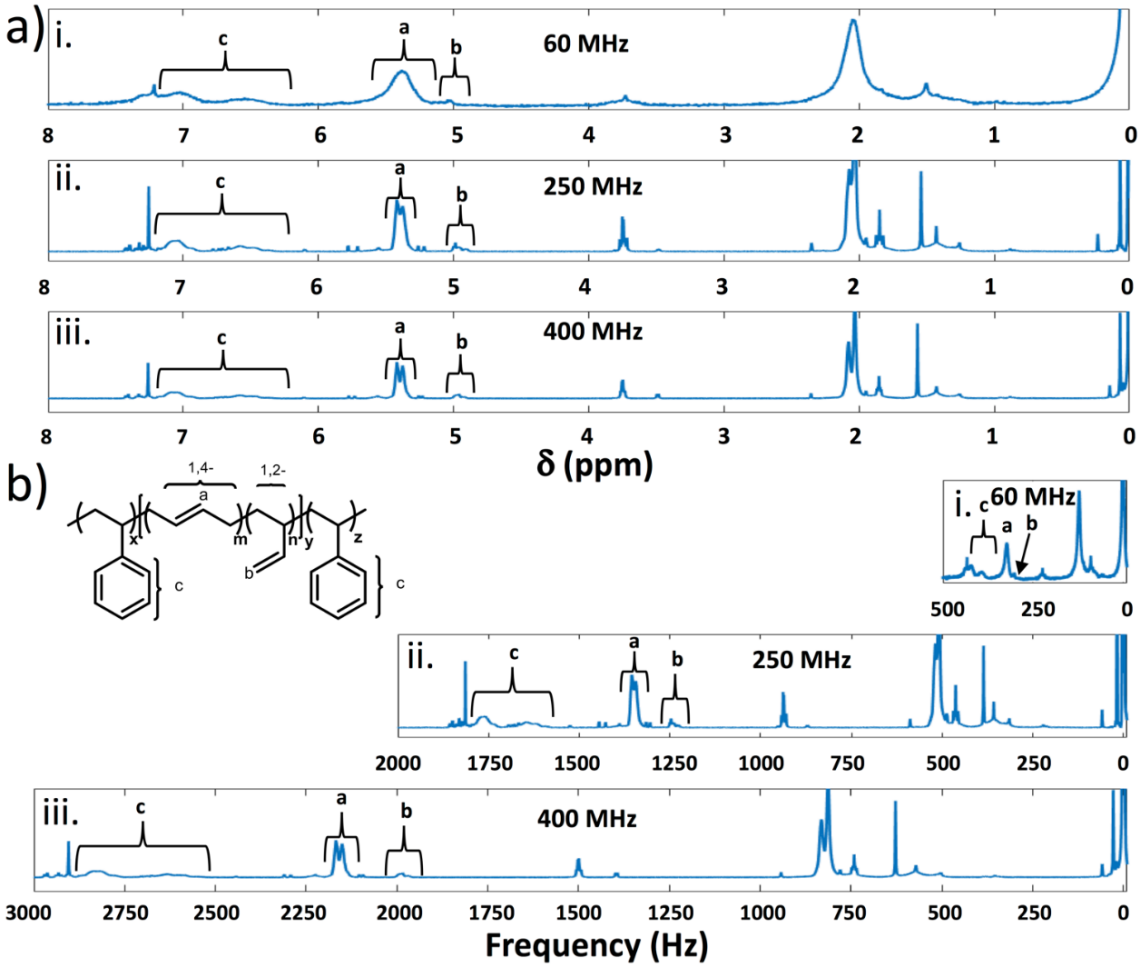

Figure 3.1. a) ^{1}H NMR spectra of SBS acquired with a i) 60 MHz spectrometer, ii) 250 MHz spectrometer, and iii) 400 MHz spectrometer. b) Frequency shift spectra of SBS acquired with i) 60 MHz spectrometer, ii) 250 MHz spectrometer, and iii) 400 MHz spectrometer.

In the analysis of multicomponent polymer systems, Singh and Blümich recently investigated the ability of a 43 MHz (1 T) compact NMR spectrometer outfitted with both ^{1}H and ^{13}C probes for quality control of styrene-butadiene rubber (SBR) production.[31] By using 1D ^{1}H and ^{13}C spectra in combination with a partial least squares regression they found they could determine the S/B relative composition and the polybutadiene microstructure quantitatively.[31] Additionally, they were able to distinguish differences within lots and across production processes and suppliers as a proof of concept of this approach for quality control in industrial SBR production.[31] However, the total acquisition time for each sample was quite long – 1 minute and 5.7 hours for ^{1}H and ^{13}C spectra acquisition respectively—and a multivariate calibration model which calibrates for the prediction of composition in unknown samples from known samples.[31] These complexities may hinder application such that a faster and model-free process would be desirable. For our primary purposes in the synthesis and characterization of various polymers, statistical copolymers and block copolymers, accurate characterization of copolymer composition and microstructure is paramount and so we set out to benchmark low-field ^{1}H NMR for composition and microstructural analysis.

In this Chapter, the utility of low-field 1D ^{1}H NMR spectroscopy as a stand-alone technique for quantitative molecular characterization of a set of polymer blends and block copolymers, is investigated. In particular, the following are investigated: (1) microstructure analysis of polyisoprene (2) compositional and polydiene microstructural analysis of commercially available poly(styrene-*b*-isoprene-*b*-styrene) (SIS) and poly(styrene-*b*-butadiene-*b*-styrene) (SBS) triblock copolymers, and (3) compositional analysis of a series of polystyrene/polyisoprene (PS/PI) and polystyrene/poly(methyl methacrylate) (PS/PMMA) polymer blends as proxies for statistical and block copolymer analysis. The ability to conduct routine analyses of polymer blends such as these and copolymers at comparatively low cost in-house has potential implications for polymer instrumentation in academic and industrial research laboratories as well as industrial implications

in quality control scenarios. The chemical structures of the four polymers examined in this work are shown in Figure 3.2.

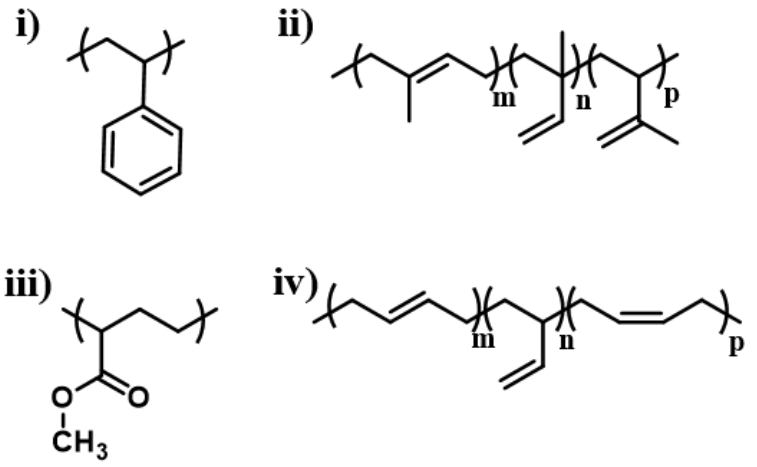

Figure 3.2 Chemical structures of i) polystyrene, ii) polyisoprene, iii) poly (methyl methacrylate), and iv) polybutadiene.

3.2 Experimental details

3.2.1 Materials

Styrene, cyclohexane, deuterated chloroform and tetramethylsilane (TMS) were purchased from EMD Millipore Corporation. Isoprene was obtained from Acros Organics. Tetramethylethylenediamine, polystyrene-*b*-polyisoprene-*b*-polystyrene (SIS) symmetric triblock copolymer (catalog # 432415), polystyrene-*b*-polybutadiene-*b*-polystyrene (SBS) (catalog # 43249-0), *sec*-Butyllithium and 2,2'-azobis(2-methylpropionitrile) were used as received from Sigma Aldrich. 1,1 diphenylethylene, *n*-butyllithium and inhibitor removal column resin (catalog # 42489) were procured from Alfa Aesar. Methanol and Chloroform were obtained from VWR International and *tert*-Butyllithium was received from TCI America. Cyclohexane was stirred over diphenylhexyllithium (adduct of *sec*-butyllithium and 1,1-diphenylethylene), degassed via freeze-pump-thaw (FPT) cycles, and vacuum transferred prior to use. Isoprene was stirred over *n*-butyllithium, degassed via FPT, and vacuum transferred prior to use. *Caution! sec-butyllithium and*

n-butyllithium are pyrophoric and moisture-sensitive materials and should be handled with appropriate care. Styrene and methyl methacrylate were passed through the inhibitor removal column and degassed by FPT cycles prior to use. Methanol, for terminating the anionic polymerization of isoprene, was degassed via FPT cycles prior to use.

3.2.2 Polymer Synthesis

All reactors were flamed out under vacuum. *tert*-butyllithium initiated anionic polymerization of isoprene was performed at 60 °C. *Caution! tert-butyllithium is a pyrophoric and moisture-sensitive material and should be handled with appropriate care.* Cyclohexane, isoprene and *tert*-butyllithium were charged to a reactor in a nitrogen-filled glovebox prior to removal and heating to 60 °C by submersion in a temperature-controlled water bath. Upon completion the polymerization was terminated with degassed methanol. Polystyrene (PS) and poly(methyl methacrylate) (PMMA) were synthesized by free radical polymerization at 70 °C, neat, using 2,2'-azobis(2-methylpropionitrile) (AIBN) as the initiator. AIBN and monomer were charged to a reactor in a nitrogen-filled glovebox prior to removal and heating to 70 °C by submersion in a temperature-controlled water bath. Upon completion the polymers were removed from the water bath, precipitated in methanol and the product collected and dried in a vacuum oven.

3.2.3 Instrumentation

Two NMR spectrometers were primarily used in this study to obtain ^{1}H NMR spectra. Spectra at 400 MHz (9.4 T) were collected on a Bruker Avance 400 spectrometer and spectra at 60 MHz (1.4 T) were collected on an Oxford Instruments Pulsar 60 MHz spectrometer. The spectrum at 250 MHz shown in Figure 1 was collected on a Bruker Avance II 250 MHz spectrometer.

3.2.4 Polymer Blend Preparation and Characterization

PS/PI and PS/PMMA polymer mixtures of varied relative composition were prepared gravimetrically, dissolved in deuterated chloroform to 10-50 mg/mL (maintaining the minority

constituent concentration at 5 mg/mL) and doped with 1-2 drops of TMS for analysis. At 400 MHz, 16 scans were collected at room temperature in 1.32 minutes using standard sample parameters unless otherwise noted. At 60 MHz, 128 scans were collected in 19.82 minutes using a relaxation delay of 2 seconds between scans, unless otherwise noted. The 60 MHz spectrometer internal temperature was 37 °C and the 400 MHz spectrometer internal temperature was 19 °C. Free induction decays (FIDs) were Fourier-transformed, manually phase-corrected and the chemical shift calibrated relative to the TMS peak prior to peak integration using MNOVA.

3.3 Results and Discussion

3.3.1 Polyisoprene microstructural characterization

Polymers such as polyisoprene (PI) and polybutadiene (PB) are essentially copolymer structures due to the different modes of addition during polymerization; 1,4-, 1,2-, and 3,4-polyisoprene and 1,2- and 1,4-polybutadiene. We synthesized polyisoprene in cyclohexane using anionic polymerization to yield a high 1,4-content polyisoprene analogous to that typically present in commercially available SIS triblock copolymers. The polyisoprene product was dissolved in deuterated chloroform, doped with TMS and analyzed using ^{1}H NMR spectroscopy at both 400 MHz and 60 MHz (Figure 3.3). Comparing the spectra in Figure 3.3, clearly distinguishable peaks are observed in both with the 60 MHz spectra peaks appearing broader, less defined, with slight overlap.

As mentioned above, the sharpness and contrast of the peaks is directly dependent on both field strength and the number of scans. By increasing the number of scans and thereby improving the signal-to-noise ratio (Equation 3), spectra quality improves visually as shown in Figure 3.4a. Of interest for polyisoprene microstructural characterization are the peaks at 4.7 ppm, 5.1 ppm, and 5.7 ppm corresponding to 3,4-, 1,4- & 1,2- addition respectively. Based on these peak areas, the microstructure can be determined. In both the 400 MHz and 60 MHz spectra no 1,2-PI content is

observed, i.e. no peak at 5.7 ppm, as expected for the synthetic route chosen. In the absence of 1,2-PI, the 1,4- and 3,4-content can be calculated directly from the peaks at 4.7 ppm and 5.1 ppm according to equations (3.4) and (3.5), where I_i is the area of the peak at *i* ppm, yielding the results shown in Figure 3.4b.

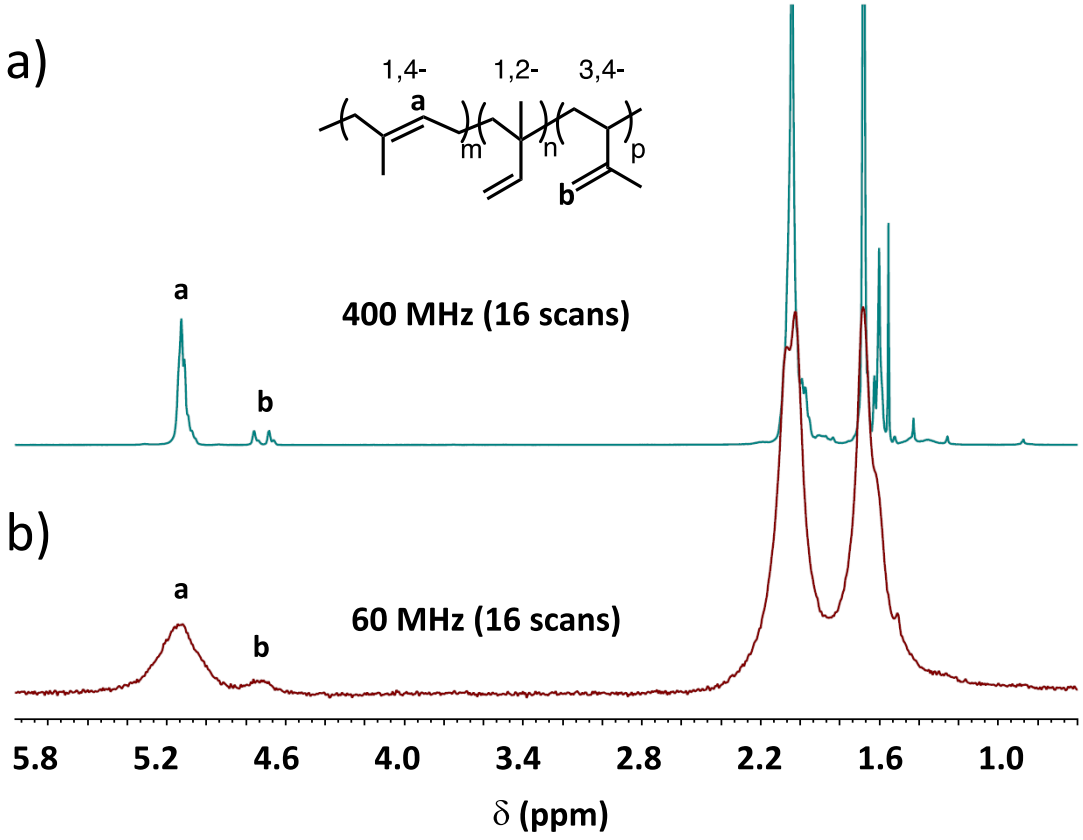

Figure 3.3 ^{1}H NMR spectrum of PI acquired at a) 400 MHz and b) 60 MHz.

$$\%1,4\ (=CH-) = 100 * \frac{I_{5.1}}{I_{5.1} + \frac{I_{4.7}}{2}} \tag{3.4}$$

$$\%3,4\ (=CH_2) = 100 * \frac{\frac{I_{4.7}}{2}}{I_{5.1} + \frac{I_{4.7}}{2}} \tag{3.5}$$

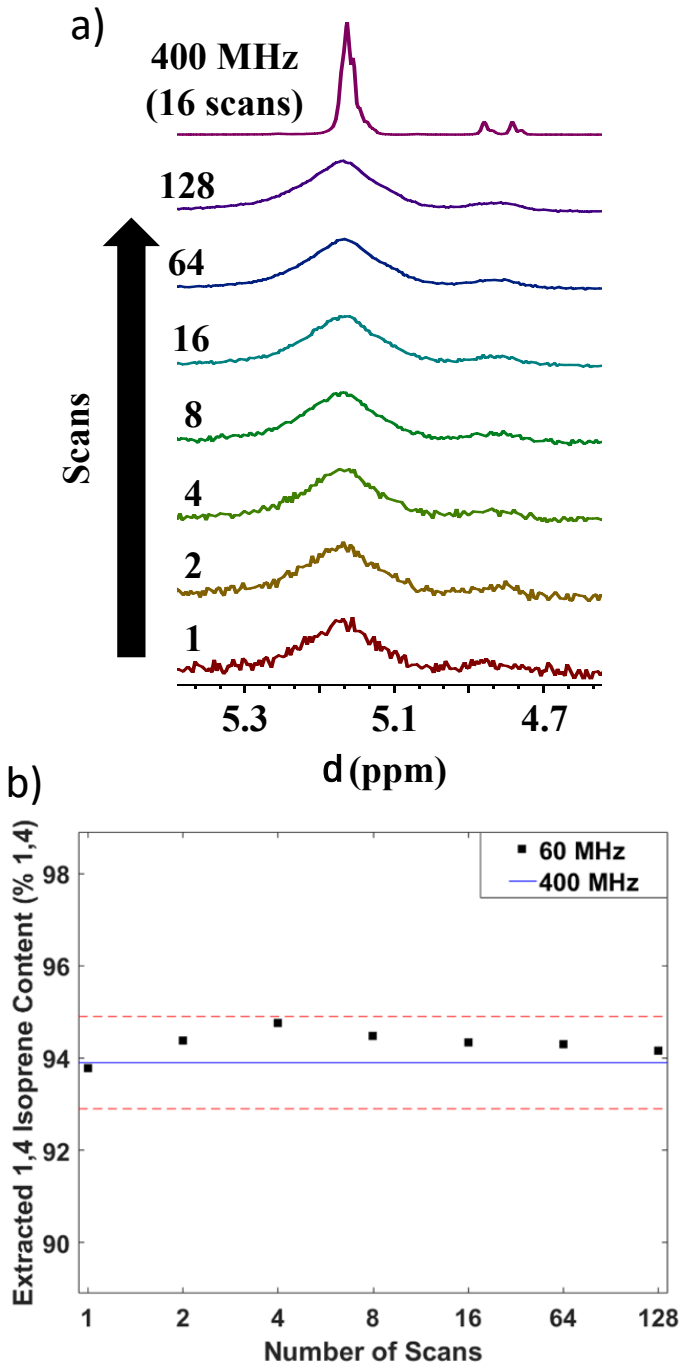

Figure 3.4 (a) Polyisoprene high-field ^{1}H NMR spectrum acquired at 400 MHz (top) compared to 60 MHz spectra of varied number of scans. (b) Polyisoprene microstructure (% 1,4-addition) obtained from 60 MHz spectra at varied number of scans. The solid horizontal line indicates the % 1,4-addition obtained from the 400 MHz spectrum with dotted horizontal lines indicating ±1% around the 400 MHz value.

As shown in Figure 3.4b, excellent agreement is obtained, within 1%, between the 60 MHz and 400 MHz spectra. For instance, at the same number of scans as a typical high-field experiment (16 scans), we find excellent agreement between the 60 MHz (94.3% 1,4-PI) and 400 MHz (93.9% 1,4-PI) results. As relative polymer compositions are typically rounded to the nearest percent, 94% 1,4-polyisoprene is extracted from both spectra. Notably, even at a single scan excellent agreement is achieved even though the spectrum is considerably noisier. Overall, we find the 60 MHz spectrometer capable of performing this characterization quantitatively as desired.

3.3.2 Symmetric triblock compositional analysis

The block copolymers, SBS and SIS are commercially available thermoplastic elastomers and utilized in a wide variety of applications from footwear to asphalt modification. Here, SBS and SIS triblock copolymers are purchased from Sigma Aldrich, dissolved in deuterated chloroform, and doped with TMS and ^{1}H NMR spectra were obtained at both 400 MHz and 60 MHz. Both ^{1}H NMR spectra are shown in Figure 3.5 for SIS and Figure 3.6 for SBS.

At 400 MHz clear distinct peaks are obtained, whereas at 60 MHz peaks appear broader and less defined. Both the polydiene microstructure and the relative composition of styrene and diene are extracted from the spectra. For SIS, the peak regions for the polystyrene aromatic protons (6.3–7.2 ppm) and the polyisoprene allylic protons (4.7 ppm, and 5.1 ppm) are integrated and the microstructure and composition determined for SIS using equation (3.4) – (3.6).

$$\%S(in\,SIS) = 100 * \frac{\frac{I_7}{5}}{I_{5.1} + \frac{I_{4.7}}{2} + \frac{I_7}{5}} \tag{3.6}$$

The composition of SBS was determined using the same process as the SIS (Equation 6) using Equation 7 and the PB microstructure (1,2- and 1,4-content) was determined the same process as the PI microstructure (Equations 3.4 and 3.5) using Equations 3.8 and 3.9.[6, 8]

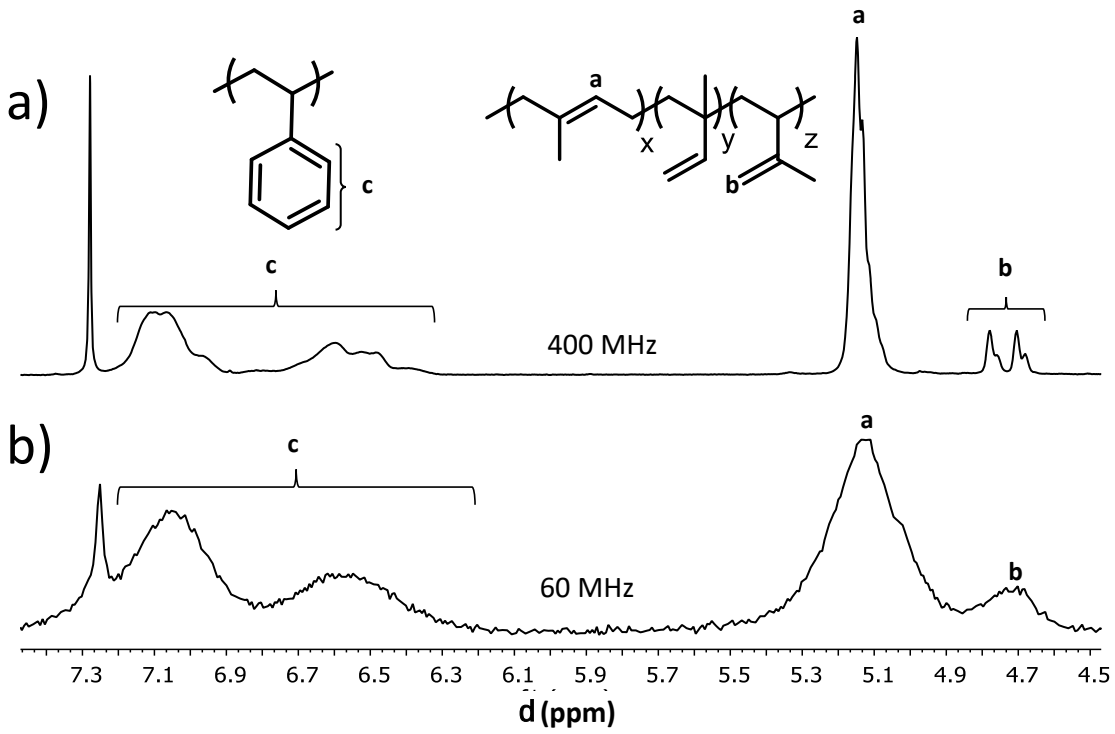

Figure 3.5 [1]H NMR spectra of SIS triblock copolymer at a) 400 MHz and b) 60 MHz

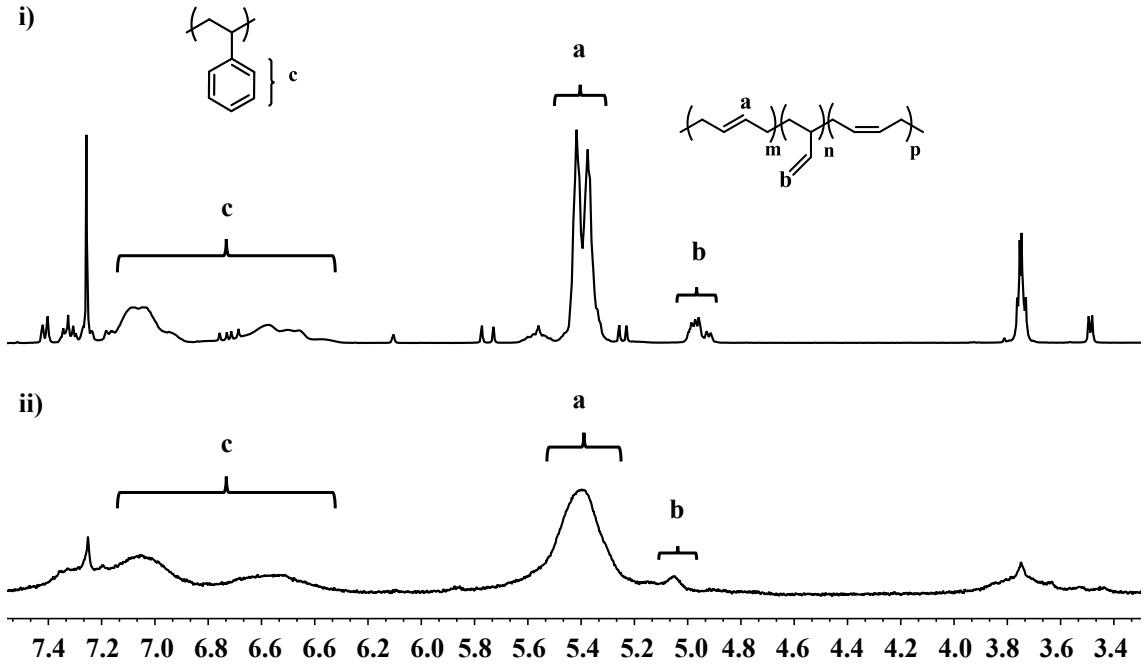

Figure 3.6 [1]H NMR spectra of SBS triblock copolymer at i) 400 MHz and ii) 60 MHz.

$$\%S(in\,SBS) = 100 * \frac{\frac{I_7}{5}}{I_{5.4} + I_{5.6} + \frac{I_7}{5}} \tag{3.7}$$

$$\%1,2\ (= CH_2) = 100 * \frac{I_{5.6}}{I_{5.4} + I_{5.6}} \tag{3.8}$$

$$\%1,4\ (= CH-) = 100 * \frac{I_{5.4}}{I_{5.4} + I_{5.6}} \tag{3.9}$$

The spectrum acquired at 60 MHz again clearly possesses adequate capability to detect polystyrene peaks at 6.2–7.3 ppm, as well as both 1,4- and 3,4-polyisoprene configurations and no 1,2-content (5.7 ppm) is visible in either spectrum. Using the polydiene microstructures and polystyrene content obtained at 400 MHz as the "true" value, we find excellent agreement. Both SBS and SIS are high in 1,4-content as expected for these commercial triblock copolymers, which are typically synthesized via anionic polymerization in hydrocarbon solvents. For SBS, we find a composition of 10.1% styrene with 95.4% 1,4-polybutadiene using the 400 MHz spectra, while the 60 MHz spectra yield 12.2% styrene with 98.7% 1,4-polybutadiene. At 400 MHz we determine the SIS to be 16.4% polystyrene with 94.3% 1,4-polyisoprene compared to 15.5% polystyrene with 92.9% 1,4-polyisoprene at 60 MHz. This is excellent agreement as, generally, the confidence in compositional analysis performed using high-field NMR spectrometers in this manner for polymers is ±1%. Here, the 60 MHz results fall within this typical experimental confidence for SIS while SBS is just outside with a 2% difference in composition. Overall, the 60 MHz results are quantitatively the same for SIS with slight deviation for SBS. This level of accuracy at lower cost and increased accessibility could find use for quality control, research characterization and other applications and is acceptable for validating the use of these low-field instruments for this analysis.

3.3.3 Polymer Blend Compositional Analysis

To assess the utility of low-field ^{1}H NMR spectroscopy for the compositional analysis of polymer blends and other block copolymer systems, polystyrene and poly(methyl methacrylate) (PMMA) were synthesized using AIBN-initiated free-radical polymerization to complement the previously discussed PI. PS/ PI and PS/PMMA mixtures were prepared gravimetrically at varied relative compositions, dissolved in deuterated chloroform to a concentration of 10–50 mg/ml as described in the Experimental section and their ^{1}H NMR spectra obtained at both 400 MHz and 60 MHz (Figures 3.7 and 3.8). The overall polymer composition for each blend was determined analogous to the triblock copolymers using the PMMA methyl protons on the acrylate side chain (3.6 ppm)[32] and the aforementioned polystyrene aromatic peaks as shown in Equation (3.10).

$$\%S(in\,PS/PMMA) = 100 * \frac{\frac{I_7}{5}}{\frac{I_{3.9}}{3} + \frac{I_7}{5}} \qquad (3.10)$$

Compositions determined using the spectra obtained with the 60 MHz spectrometer are plotted against those obtained from the 400 MHz spectrometer for both PS/PS and PS/PMMA; Figure 3.9a and 3.9b respectively (see Table 3.1 for the composition values used to construct Figure 3.9). We find excellent agreement between the 400 MHz and 60 MHz results for both PS/PI and PS/PMMA blends as nearly all points in Figure 3.9 lie along the identity line. For five of the nine PS/PI blends the compositions obtained using the 60 MHz spectra are equivalent to those from the 400 MHz spectra, after rounding to the nearest percent, with the remaining 4 differing by only 1%. Similarly, for PS/PMMA blends equivalent results are found for four of the nine blends, four differ by 1% and one differs by 2%. Overall, the average difference between the extracted compositions at 60 MHz and 400 MHz is 0.48% for PS/PI blends and 0.66% percent for PS/PMMA blends. These findings demonstrate the utility of low-field spectrometers for the quantitative determination of relative composition in these polymer blends.

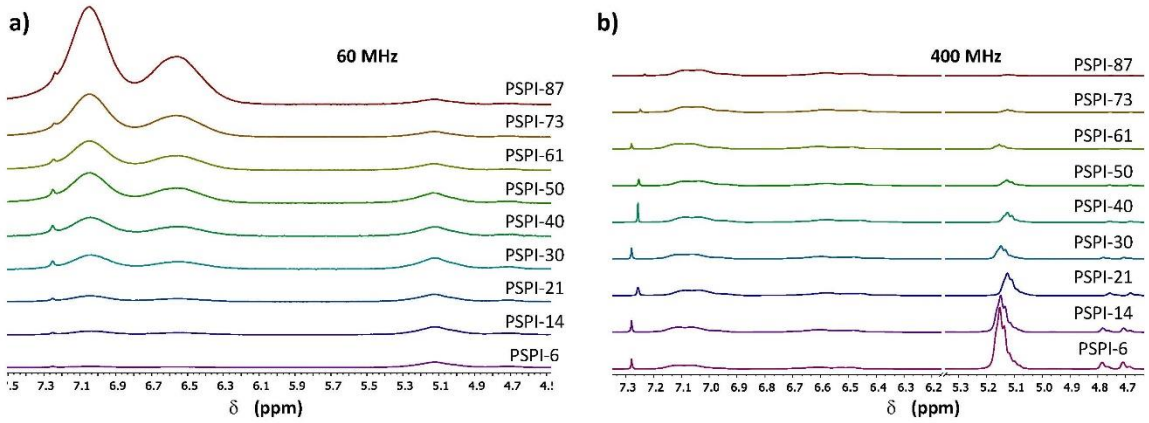

Figure 3.7 ^{1}H NMR spectra of PS/PI polymer blends at varied relative composition at a) 60 MHz and b) 400 MHz where each spectrum is named according to the PS content determined using the 400 MHz spectra for that blend.

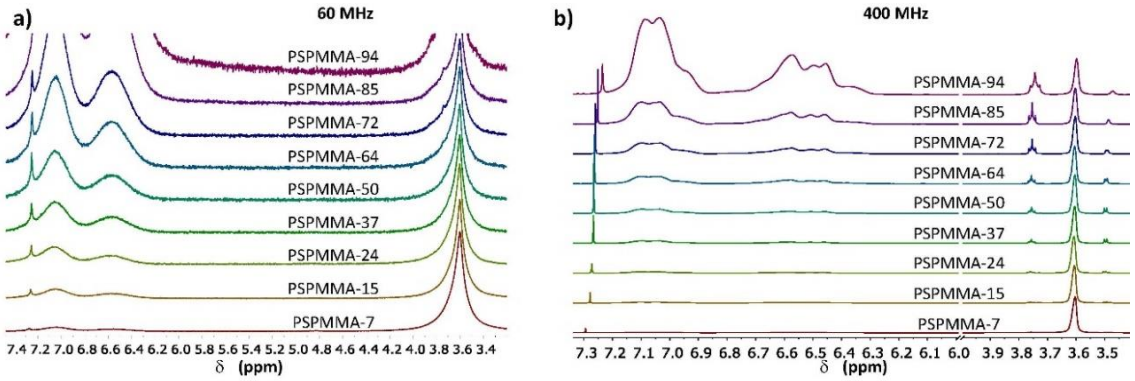

Figure 3.8 ^{1}H NMR spectra of PS/PMMA polymer blends at varied relative composition at a) 60 MHz and b) 400 MHz where each spectrum is named according to the PS content determined using the 400 MHz spectra for that blend.

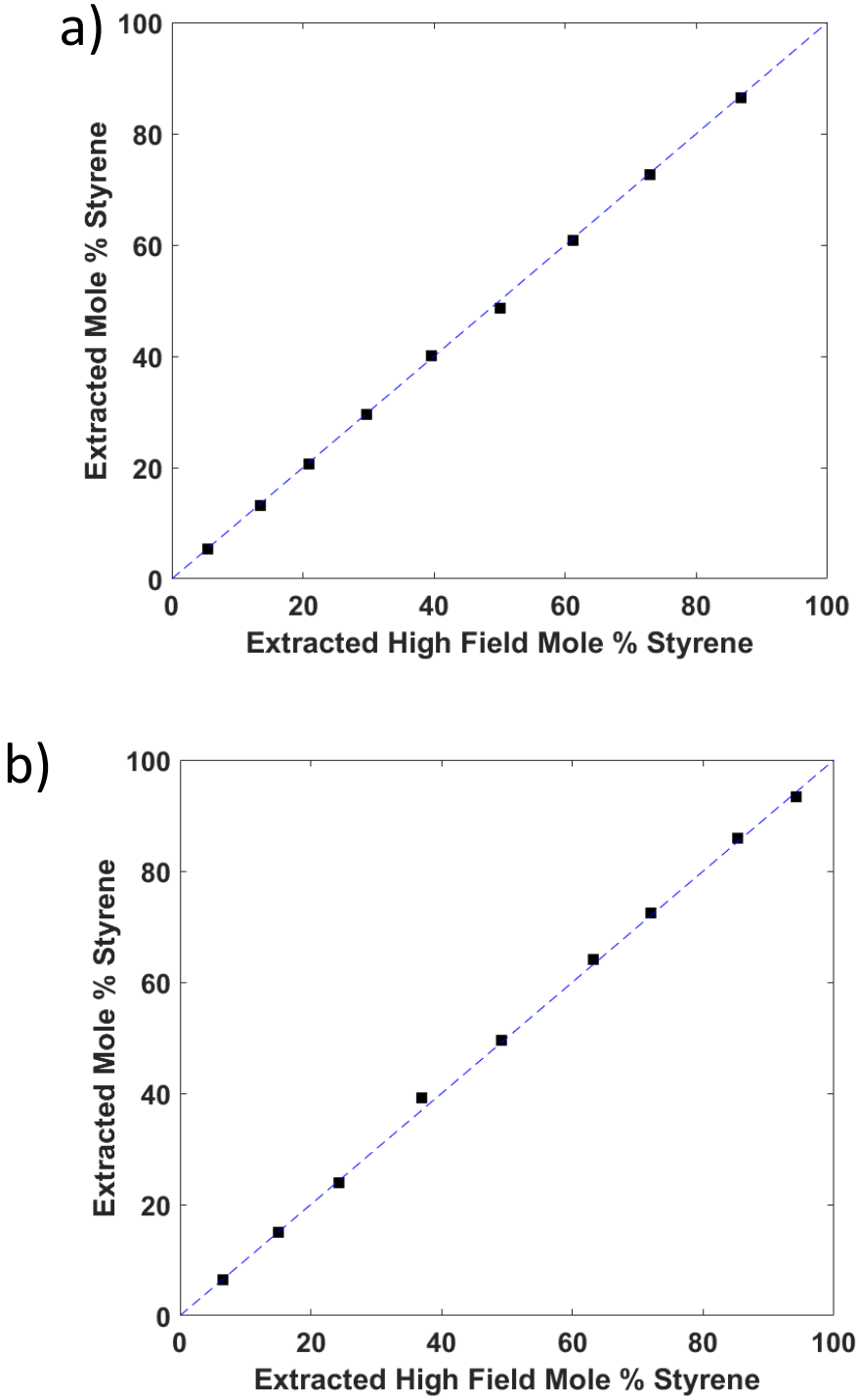

Figure 3.9 Extracted composition values from 60 MHz spectra plotted against values extracted from 400 MHz spectra for polymer blends of a) polystyrene and polyisoprene and b) polystyrene and poly(methyl methacrylate). Dashed line represents the identity line; y = x.

Table 3.1 Compositions extracted from analysis of each spectra for both PS/PI and PS/PMMA blends.

Sample	Frequency	Mole % Polystyrene	Sample	Frequency	Mole % Polystyrene
PSPI-6	60 MHz	5.4	*PSPMMA-7*	60 MHz	6.5
	400 MHz	5.6		400 MHz	6.6
PSPI-14	60 MHz	13.2	*PSPMMA-15*	60 MHz	15.0
	400 MHz	13.5		400 MHz	15.1
PSPI-21	60 MHz	20.6	*PSPMMA-24*	60 MHz	23.9
	400 MHz	20.9		400 MHz	24.3
PSPI-30	60 MHz	29.6	*PSPMMA-37*	60 MHz	39.2
	400 MHz	29.7		400 MHz	37.0
PSPI-40	60 MHz	40.0	*PSPMMA-50*	60 MHz	49.4
	400 MHz	39.6		400 MHz	49.1
PSPI-50	60 MHz	48.6	*PSPMMA-64*	60 MHz	64.1
	400 MHz	50.2		400 MHz	63.2
PSPI-61	60 MHz	60.7	*PSPMMA-72*	60 MHz	72.4
	400 MHz	61.2		400 MHz	72.0
PSPI-73	60 MHz	72.6	*PSPMMA-85*	60 MHz	86.0
	400 MHz	72.9		400 MHz	85.2
PSPI-87	60 MHz	86.4	*PSPMMA-94*	60 MHz	93.4
	400 MHz	86.8		400 MHz	94.2

3.4 Conclusions

^{1}H NMR spectroscopy is a powerful tool for the characterization of polymer structures and the relative compositions of repeat unit structures within multicomponent polymer systems. In this work the potential of a low-field spectrometer (60 MHz) to perform routine polymer characterizations; polydiene microstructure, triblock copolymer composition and polymer blend compositional analysis was assessed. While the 60 MHz spectrometer is less sensitive, with broader peaks due to the narrower frequency of acquisition, the acquired spectra possess distinct peaks containing the requisite relative concentration information for performing the desired compositional analysis. Five different polymer systems were analyzed, and the results obtained using a 60 MHz spectrometer and a 400 MHz spectrometer were compared. A majority of results

obtained for each sample using both spectrometers are within the typical experimental error anticipated for high-field spectrometers (+/- 1%). Extracted compositions are within 3% in all cases with a majority (26/31 or 84%) within 1 %. These results validate the use of 60 MHz ^{1}H NMR spectrometers for the polymer systems analyzed here. We note however that additional systems of interest should be similarly validated before application of these instruments for quantitative analyses. Overall, ^{1}H NMR spectroscopy at low-field strength is a promising tool for the routine characterization of multicomponent polymer systems.

3.5 References

(1) Krishnamoorti, R.; Graessley, W. W.; Dee, G. T.; Walsh, D. J.; Fetters, L. J.; Lohse, D. J. *Macromolecules* **1996**, *29*, 367–376.

(2) Wu, S. *Polymer (Guildf).* **1985**, *26*, 1855–1863.

(3) Coleman, M. M.; Painter, P. C. *Progress in Polymer Science*. 1995, pp 1–59.

(4) Barlow, J. W.; Paul, D. R. *Polym. Eng. Sci.* **1981**, *21* (15), 985–996.

(5) L. A. Utracki; C. Wilkie. *Polymer Blends Handbook*; Springer, 2014.

(6) Tanaka, Y.; Takeuchi, Y.; Kobayashi, M.; Tadokoro, H. *J. Polym. Sci. Part A-2 Polym. Phys.* **1971**, *9* (1), 43–57.

(7) Stuart, B. *Polymer Analysis*; Wiley, 2008; Vol. 9783527336.

(8) Santee, E. R.; Chang, R.; Morton, M. *300 MHz proton NMR of polybutadiene: Measurement of cis-trans isomeric content*; 1973; Vol. 11.

(9) Kovacs, H.; Moskau, D.; Spraul, M. *Prog. Nucl. Magn. Reson. Spectrosc.* **2005**, *46* (2–3), 131–155.

(10) H. Gunther. *NMR Spectroscopy: Basic Principles, Concepts and Applications in Chemistry*; Wiley, 1995.

(11) Spiess, H. W. *Macromolecules* **2017**, *50*, 1761–1777.

(12) Blümich, B. *TrAC - Trends Anal. Chem.* **2016**, *83*, 2–11.

(13) Adams, A. *Trends Anal. Chem.* **2016**, *83*, 107–119.

(14) Donaldson, M.; Freed, D.; Mandal, S.; Song, Y. Q. *TrAC - Trends Anal. Chem.* **2016**, *83*, 84–93.

(15) Nordon, A.; Gemperline, P. J.; McGill, C. A.; Littlejohn, D. *Anal. Chem.* **2001**, *73*, 4286–4294.

(16) Hertlein, C.; Saalwächter, K.; Strobl, G. *Polymer (Guildf).* **2006**, *47* (20), 7216–7221.

(17) Eccles, C. *Low Field NMR Methods and Applications*; 2010.

(18) Dalitz, F.; Cudaj, M.; Maiwald, M.; Guthausen, G. *Prog. Nucl. Magn. Reson. Spectrosc.* **2012**, *60*, 52–70.

(19) Parker, T.; Limer, E.; Watson, A. D.; Defernez, M.; Williamson, D.; Kemsley, E. K. *Trends Anal. Chem.* **2014**, *57*, 147–158.

(20) Isaac-Lam, M. F.; F., M. *Int. J. Spectrosc.* **2016**, *2016*, 1–8.

(21) Jakes, W.; Gerdova, A.; Defernez, M.; Watson, A. D.; McCallum, C.; Limer, E.; Colquhoun, I. J.; Williamson, D. C.; Kemsley, E. K. *Food Chem.* **2015**, *175*, 1–9.

(22) Ruan, R. R.; Long, Z.; Song, A.; Chen, P. L. *LWT - Food Sci. Technol.* **1998**, *31*, 516–521.

(23) Elipe, M. V. S.; Milburn, R. R. *Magn. Reson. Chem.* **2016**, *54* (6), 437–443.

(24) Pedroza, O. J. O.; Tavares, M. I. B.; Preto, M. *Polym. Test.* **2006**, *25* (2), 246–248.

(25) Preto, M.; Tavares, M. I. B.; Silva, E. P. d. *Polym. Test.* **2007**, *26* (4), 501–504.

(26) Papon, A.; Saalwächter, K.; Schäler, K.; Guy, L.; Lequeux, F.; Montes, H. *Macromolecules* **2011**, *44* (4), 913–922.

(27) Patel, J. P.; Hsu, S. L. *J. Polym. Sci. Part B Polym. Phys.* **2018**, *56* (8), 639–643.

(28) Cudaj, M.; Guthausen, G.; Hofe, T.; Wilhelm, M. *Macromol. Chem. Phys.* **2012**, *213* (18), 1933–1943.

(29) Cudaj, M.; Guthausen, G.; Hofe, T.; Wilhelm, M. *Macromol. Rapid Commun.* **2011**, *32* (8), 665–670.

(30) Höpfner, J.; Ratzsch, K. F.; Botha, C.; Wilhelm, M. *Macromol. Rapid Commun.* **2018**, *39* (7), 1–7.

(31) Singh, K.; Blümich, B. *Polymer (Guildf).* **2018**, *141*, 154–165.

(32) Nagai, M.; Nishioka, A. *J. Polym. Sci. Part A-1 Polym. Chem.* **1968**, *6* (6), 1655–1660.

CHAPTER 4: TUNING THE COMPOSITIONAL DRIFT - ANIONIC LIVING COPOLYMERIZATION OF STYRENE AND ISOPRENE

This chapter details the synthesis of various copolymers of styrene and isoprene of varied architecture by varying the solvent environment. Copolymer syntheses were performed in cyclohexane as well as varying volumetric ratios of cyclohexane and triethylamine. Copolymerization reactions are monitored in-situ in order to track the compositional drift using Attenuated-Total-Reflectance Fourier Transform Infrared (ATR-FTIR) spectroscopy. Copolymerization behavior is quantified through reactivity ratio analysis and relationships between reaction environment and copolymer structure extracted. The final copolymer products are characterized using ^{1}H NMR, GPC and DSC and the results are reported.

4.1 Introduction

The chemistry of polymer chains has a colossal impact on the properties of the bulk polymer. Thus, controlling the way in which monomers are incorporated into polymer chains during copolymerization, would enable synthesizing polymers with specific and desired properties. In radical copolymerizations that are generally indiscriminate to solvent environment, control over monomer incorporation cannot easily be achieved.[1] However, anionic polymerization is more sensitive to variations in temperature, solvent environment, ionic character and so on, thereby allowing greater control over monomer relative reactivity. Anionic living copolymerizations are customarily characterized by the presence of a compositional gradient along the chain.[1] This compositional gradient in living chain copolymerizations is directly related to the relative reactivity (i.e. reactivity ratios) of the monomers involved. The different kinds of compositional architectures

(random, block, alternating or gradient) that result from copolymerization can be distinguished by the nature of the reactivity ratio values (Figure 4.1) which are representative of the tendency of the propagating chain end to react and enchain the same type of monomer which is at its terminal end over the other monomer involved.[2] These reactivity ratios are specific to the monomer pairs under distinct reaction conditions, like temperature, type of solvent or presence of additives. Thus, since reactivity ratios herald the trend of the compositional drift as a result of the differences in monomer reactivity, they are widely used to differentiate between the four important types of copolymerization behavior – random, blocky, gradient and alternating as shown in Figure 4.1b.[3]

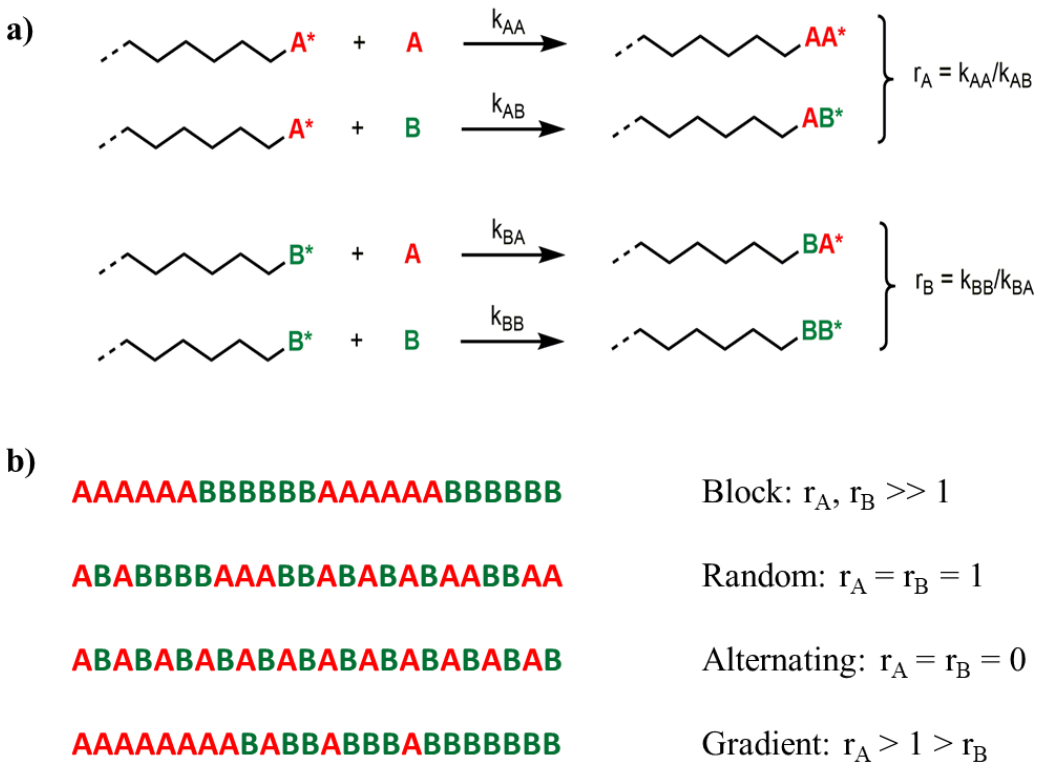

Figure 4.1 Schematic representation of the types of copolymers based on the values of reactivity ratios of monomers (adapted from Beckingham, Sanoja and Lynd[4])

The terminal model of copolymerization has extensively been in use to describe the instantaneous copolymer composition (or the compositional drift) of copolymerizations.[3,5,6] As per this model,

the chemical reactivity of the growing chain in a particular environment depends on only the identity of the repeat unit at the propagating chain end and the identity of the monomer adding to the chain as shown in Figure 4.1a. Considering the case of copolymerization of two monomers A and B, this model results in four propagation rate constants, k_{AA}, k_{AB}, k_{BB} and k_{BA}, which fully describe the copolymerization kinetics. The reactions depicted in Figure 4.1a coupled together with the necessary initiation step can be used to generate a system of ordinary differential equations (ODEs) which describe the kinetics of chain copolymerization; Equations 4.1 and 4.2, where *A(t)*, *B(t)* and *X(t)* are the time-dependent concentrations of monomer A, monomer B and initiator X, *A*(t)* and *B*(t)* are the time dependent concentrations of polymer chains with terminal species A and B; and k_X and k_{XB} are the respective rate constants of initiation of monomer A and monomer B.[4]

$$-\frac{dA}{dt} = k_{AA}A(t)A^*(t) + k_{BA}A(t)B^*(t) + k_{XA}A(t)X(t) \tag{4.1}$$

$$-\frac{dB}{dt} = k_{BB}B(t)B^*(t) + k_{AB}A(t)A^*(t) + k_{XB}B(t)X(t) \tag{4.2}$$

This system of ODEs is non-linear and not solvable analytically. However, various methods have been adopted, in order to extract reactivity ratios from experimental data.[6,7,8,9] These methods by Mayo-Lewis[6], Fineman-Ross[7], Kelen-Tudos[8], and others[9] have typically used a steady-state approximation and, with the exception of Mayo-Lewis, do not integrate the underlying ODEs. The most famous representation is the so-called Copolymer Equation (or Skeist Equation) - Equation 4.3 which relates the instantaneous monomer feed (f_A or f_B) and the resultant copolymer composition (F_A)[4]:

$$F_A = \frac{r_A f_A^2 + f_A f_B}{r_A f_A^2 + 2 f_A f_B + r_B f_B^2} \tag{4.3}$$

Recently, Beckingham et al. examined a non-terminal model, where there is no reactivity dependence on the identity of the chain end (Figure 4.2).[4] In this model the reactivity of the growing chain end is only dependent on the chemistry of the monomers. Thereby, as per this model, the reactivity ratios are simplified since $k_{AA} = k_{BA} = k_A$ and $k_{BB} = k_{AB} = k_B$ (Figure 4.2) and only one propagation rate constant would be needed per monomer. This also implies that the product of reactivity ratios is equal to unity and this is a prime characteristic of ideal copolymerizations.[4]

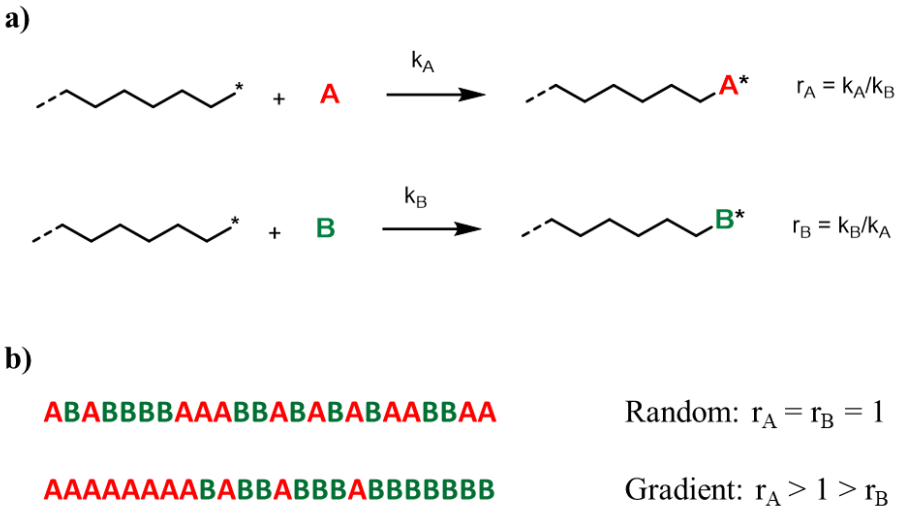

Figure 4.2 Reactivity ratios as per the non-terminal model of copolymerization which is suitable to describe random and gradient copolymerizations (figure adapted[4]).

Based on the reactions depicted in Figure 4.2a as well as the initiation steps, the kinetics of chain copolymerization for the nonterminal model can be described using a system of ordinary differential equations (ODEs) presented in Equations 4.4 – 4.6, where k_A and k_B are the respective rate constants of initiation and propagation of monomers A and B (simplified rate constants are assumed to account for initiation and propagation), A_0, B_0 and X_0 are the initial concentrations of A, B and initiator X respectively.[4]

$$-\frac{dA}{dt} = k_A A(t)\left(A^*(t) + B^*(t) + X(t)\right) = k_A A(t) X_0 \qquad B(0) = B_0 \tag{4.4}$$

$$-\frac{dB}{dt} = k_B B(t)\,(A^*(t) + B^*(t) + X(t)) = k_B B(t) X_0 \quad A(0) = A_0 \tag{4.5}$$

$$-\frac{dX}{dt} = [k_A A(t) + k_B B(t)]\, X(t) \tag{4.6}$$

This system of non-linear ODEs can be integrated using an appropriate set of initial conditions and the assumption of livingness (Equation 4.7) yielding exponentially depleting monomer concentrations (Equations 4.8 - 4.9).[4]

$$X_0 = A^*(t) + B^*(t) + X(t) \tag{4.7}$$

$$A(t) = A_0 e^{-k_A X_0 t} \tag{4.8}$$

$$B(t) = B_0 e^{-k_B X_0 t} \tag{4.9}$$

These time-dependent ODEs can be related to the compositional drift to determine the reactivity ratios. This can be done by writing out an expression for the total monomer conversion, P_{AB}, as a function of time or conversion (Equation 4.10). Here n_A and n_B are the initial mole fractions of A and B.

$$Total\,conversion = 1 - n_A \left(\frac{A(t)}{A_0}\right) - n_B \left(\frac{A(t)}{A_0}\right)^{r_B} \tag{4.10}$$

By substituting $n_B = 1 - n_A$ and substituting Equations 4.11 and 4.12 into Equation 4.10, equations that relate the compositional drift of each monomer to the reactivity ratios are derived.[4]

$$\left(\frac{A(t)}{A_0}\right) = \left(\frac{B(t)}{B_0}\right)^{r_A} \tag{4.11}$$

$$\left(\frac{A(t)}{A_0}\right)^{r_B} = \left(\frac{B(t)}{B_0}\right) \quad (4.12)$$

Ultimately, Equations 4.15 and 4.16 enable a simple way to determine the reactivity ratios for both monomers at all conversions for copolymerizations without the limitations of requiring low conversion data or a constant monomer feed composition.[4]

$$p_{AB}(p_A) = 1 - n_A(1 - p_A) - (1 - n_A)(1 - p_A)^{r_B} \quad (4.13)$$

$$p_{AB}(p_B) = 1 - n_A(1 - p_B)^{r_A} - (1 - n_A)(1 - p_B) \quad (4.14)$$

where, p_A and p_B are the conversions of the respective monomers with

$$p_A = 1 - \frac{A(t)}{A_0} \quad (4.15)$$

Tailoring the macro-scale properties of copolymers via tuning the compositional drift is a highly lucrative technique to synthesize materials for focused applications. Recently, Jaeeun Song et al[10] investigated how the degradation and subsequent release kinetics of polyether micelles using random block copolymers for applications in smart drug delivery (synthesized by anionic ring-opening polymerization) are affected when the composition of their monomers is varied. They achieved superior biocompatibility and highly tailorable release kinetics which is expected to open up a versatile avenue for smart drug delivery systems.[10] As a classical example in relation to the work presented in this chapter, is alkyllithium-initiated copolymerizations of styrene and butadiene (SB) as discussed in Chapter 2. For this system at, vastly different reactivity ratios are found depending on the solvent and temperature (cyclohexane at 25 °C vs tetrahydrofuran at -78 °C).[1] In both cases, the extreme difference in reactivity ratios leads to strong gradients such that the final polymer appears like a block copolymer. However, in cyclohexane butadiene is preferentially

added to the polymer chain, and the opposite occurs in the case of tetrahydrofuran. Gradient-free copolymers of styrene and butadiene have been achieved by Halasa et al,[11,12] using a polar modifier, however this modifier doesn't work for styrene and isoprene.[12,13] Adding potassium alkoxides to alkyllithium-initiated SB copolymerizations in hydrocarbon media has been shown to produce gradient-free poly(styrene-*r*-butadiene) (SrB) copolymers at a suitable K:Li ratio[14,15] but this hasn't been shown to yield gradient-free SI copolymers.[16,17] Kelley and Tobolsky[18] showed that for an equimolar SI copolymerization in triethylamine, an essentially gradient-free copolymer could be achieved. This work was expanded by Beckingham and Register[1], who found that a 50/50 v/v cosolvent mixture of cyclohexane and triethylamine produced gradient-free (random) copolymers across a wide range of monomer compositions while maintaining a narrow dispersity (Dispersity < 1.1).[1] Additionally, they incorporated these random copolymers within block copolymer architectures in order to investigate the resulting mixing and self-assembly behavior.[1]

In the present work, the utility of a cosolvent reaction environment of cyclohexane and triethylamine (TEA) for tuning the compositional drift between the extreme blocky nature of copolymers in neat cyclohexane and the expected flat compositional profile in 50/50 mixtures of these two solvents is examined. A series of anionic living chain copolymerizations are performed in varied cosolvent mixtures of cyclohexane and triethylamine with the monomer consumption monitored in-situ using Attenuated-Total-Reflectance Fourier Transform Infrared (ATR-FTIR) spectroscopy. Reactivity ratios are extracted for each copolymerization and the relationship between compositional drift and cosolvent character is examined. The monomer consumption data are fitted to a non-terminal model of copolymerization kinetics in accordance with the method proposed by Beckingham et al[4]. Further, the copolymers are subjected to thermal characterization using Differential Scanning Colorimetry (DSC) and molecular weight characterization using Gel Permeation Chromatography (GPC).

4.2 Experimental details

Usage of anionic initiators that are highly susceptible to termination by oxygen or moisture for anionic polymerizations requires additional care is taken in the preparation of raw materials that would be utilized for carrying out the polymerizations. Purification of solvents and monomers were performed as discussed in Chapter 2. All polymers and copolymers were synthesized in 100 mL of solvent consisting of varying volumetric ratios of cyclohexane and triethylamine, unless otherwise mentioned. All the solvent quantities and monomer ratios have been tabulated in Table 4.1 for all the copolymerizations and 1.1 mL of sec-butyllithium was used to initiate all the copolymerizations. The copolymerizations were monitored using a Mettler Toledo ReactIR15 Attenuated Total Reflectance-Fourier Transform Infrared (ATR-FTIR) spectroscopy probe system (see Figure 4.4a and 4.4b) and were carried out at ~40 °C.

To carry out the in-situ ATR-FTIR monitored anionic copolymerizations, the required quantities of cleaned solvents, cleaned monomers and initiator, sec- Butyllithium (with 5 mL of cyclohexane) were syringe transferred into three separate air-tight glass burettes within a nitrogen-filled glovebox. A custom-built five-port glass reactor with the ATR-FTIR spectroscopy probe inserted, was purged with nitrogen through a custom adapter connected to the nitrogen manifold of a Schlenk line. The reactor was maintained at the desired temperature (~40 °C) using a water bath. The three burettes were fitted onto the reactor and the nitrogen flow was decreased. The reactor was then evacuated by connecting to the vacuum manifold of the Schlenk line to about 150 mtorr before sealing from the Schlenk line and commencing spectral acquisition at one-minute time intervals. Solvent, monomer and then initiator were charged into the reactor with at least 5 ATR-FTIR spectra acquired between subsequent additions to ensure stable spectra for solvent subtraction at the reactor temperature ~40 °C. Once complete, the polymerization was terminated by injecting an adequate quantity of degassed methanol into the reactor through a septum located on the custom Schlenk adapter. A sample of the final reaction mixture was immediately transferred to an NMR

tube and analyzed using an Oxford Instruments Pulsar 60 MHz ^{1}H NMR spectrometer to extract the solvent composition, the final styrene and isoprene content of the copolymers as well as the microstructure of the copolymers, and to verify that there are no remaining monomers present in the reaction mixture (i.e., to verify 100% conversion). The copolymerizations were terminated using degassed methanol by monitoring the attenuating signal from monomers at their specific wavelengths shown by the iCIR 7 software. The copolymers were precipitated in adequate quantities of methanol, dried under nitrogen and in the vacuum oven before running them on DSC and GPC for thermal and molecular characterization. The final copolymers were also run on the 600 MHz Avance II for compositional and microstructural analysis since 1,2 contents were expected in most of the copolymers and the low-field instrument is inadequate to detect the low 1,2 contents.

The acquired spectra from the ATR-FTIR were baselined to account for thermal drift and the acquired solvent mixture spectra was subtracted using Mettler Toledo's iCIR7 software. The polymerization conversion was monitored by tracking the styrene and isoprene monomer peaks at wavenumbers of about 1633 cm^{-1} and 1599 cm^{-1} respectively in order to ensure the complete conversion of both the monomers before termination.[19]

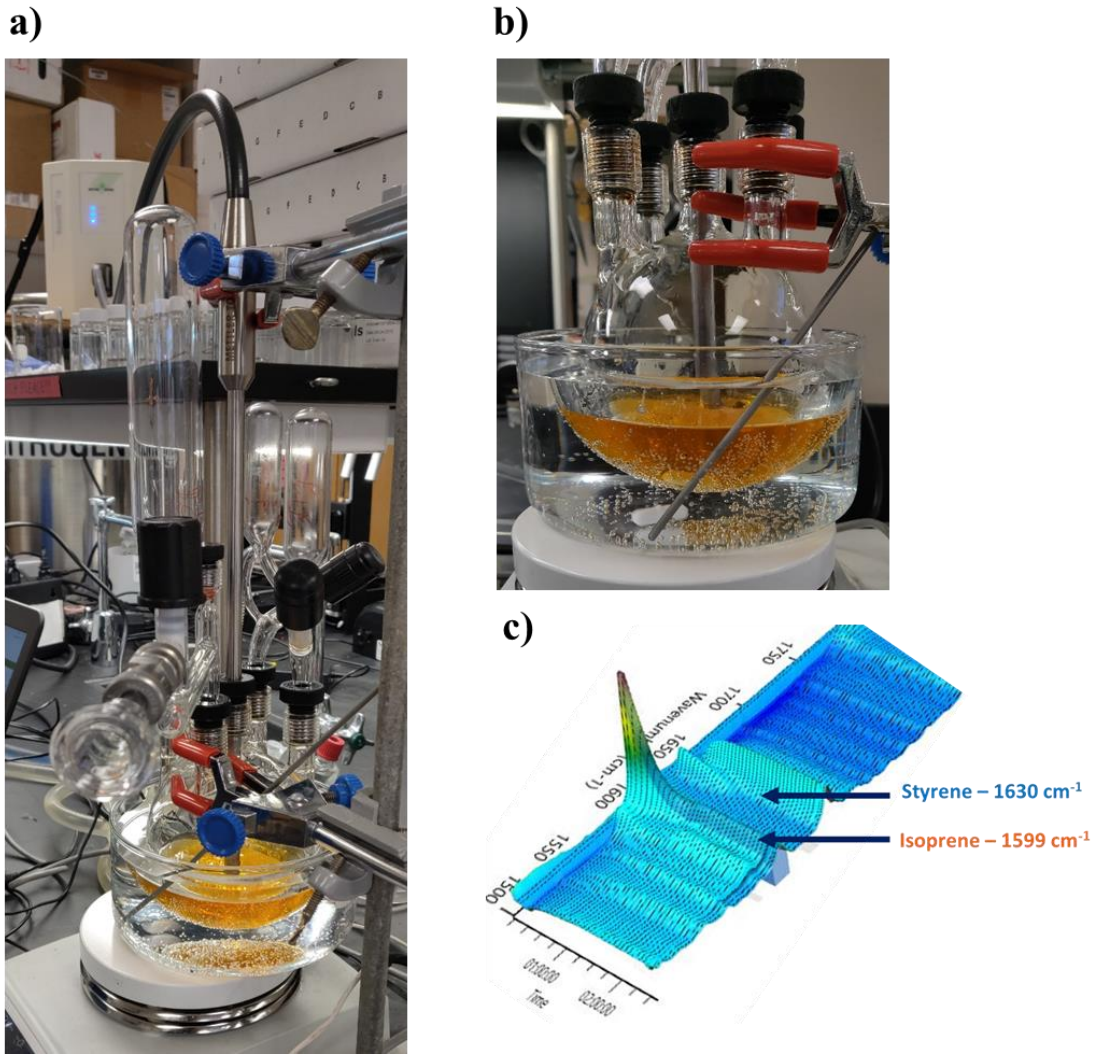

Figure 4.3 (a) The experimental setup with ATR-FTIR control unit and optical reflectance cable seen in the backdrop, (b) The ATR-FTIR probe tip immersed in the copolymerization medium, (c) A 3D plot (of time versus absorption and wavenumber) zoomed to the region of interest (1599 – 1633 cm^{-1}) depicting monomer consumption as a function of time obtained using iCIR 7 software for the SI-40/31 copolymer.

4.3 Results and Discussion

Distinct copolymerizations were carried out by varying the triethylamine content between 0 % to 50 % in the co-solvent mixture with cyclohexane. All these copolymerizations were monitored in-situ using ATR-FTIR spectroscopy by tracking the consumption of monomers and terminating them after ensuring the complete consumption of both the monomers. The synthesized copolymers along with some characterization details are systematized into Table 4.1. In the naming of the copolymers, 'SI' refers to the fact that they are composed of styrene and isoprene; the first number represents the volume percent of TEA in the solvent and the second number is the mole percent polystyrene in the copolymer. For example, SI-0/29 was synthesized in pure cyclohexane (0 % triethylamine) and consists of 29 mol % of styrene units.

All the reported copolymerizations were successfully monitored using in-situ ATR-FTIR spectroscopy and the consumption of monomers determined by tracking the signals at wavenumbers specific to both the monomers. The distinct band region for styrene at 1633 cm^{-1} corresponds to the vinylic C=C stretching in styrene.[19] Due to the effects of a growing peak that was partially overlapping at 1633 cm^{-1} in our case, we opted to use the region at 1630 cm^{-1} instead. At 1630 cm^{-1}, the styrene monomer consumption could be clearly tracked. On the other hand, 1599 cm^{-1} corresponds to the C=C stretching in isoprene and was chosen for isoprene without complications.[19] The acquired absorption spectra were baselined to account for thermal drift and the acquired solvent subtraction was carried out using iCIR 7. Figure 4.4 shows the absorption data plotted against time for SI-40/34. Similar trends of decreasing absorption signal versus time at the chosen wavelengths for styrene and isoprene are displayed by the iCIR software all through the progress of the copolymerization which aids in the termination of the copolymerizations as the trend flattens out (which indicates complete monomer conversion). Note that, SI-28/31 and SI-29/26 as well as SI-40/31 and SI-41/31 were synthesized as replicates with respect to their triethylamine content and copolymer composition.

Table 4.1 A summary of details of initiation temperature, copolymerization cosolvent and copolymer compositions.

Polymer	Temperature of initiation (°C)	Volume % TEA	Mol % Styrene	Mol % 1,4	Mol % Vinyl 3,4 (1,2)
SI-0/29	39	0	29	96	4 (0)
SI-9/28	39	9	28	71	27 (1)
SI-28/31	41	28	31	60	40 (1)
SI-29/26	43	29	26	63	36 (1)
SI-40/31	40	40	31	59	40 (1)
SI-41/31	38	41	31	58	41 (1)
SI-50/26	40	50	26	59	39 (2)

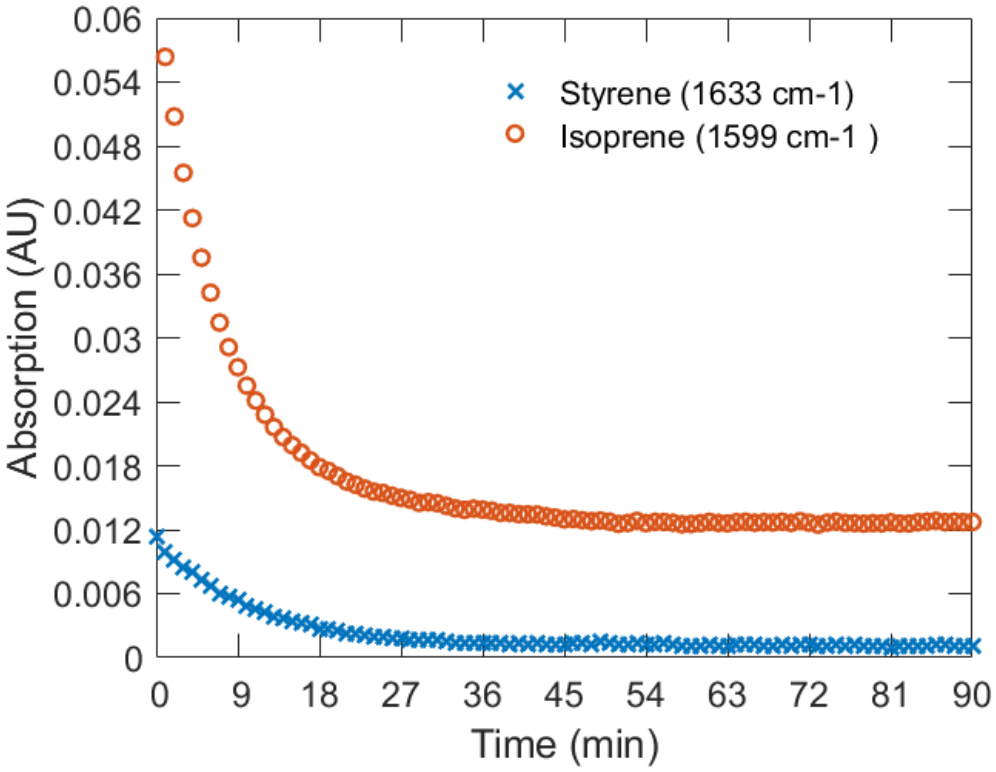

Figure 4.4 Absorption data from ATR-FTIR plotted against time for SI-40/31.

The 1,4 content of isoprene units is seen to decrease with the increasing content of TEA in the solvent mixture, while the content of 3,4 and 1,2 units increase. The final copolymers were run on the 600 MHz Avance II for compositional and microstructural analysis since 1,2 contents were

expected in most of the copolymers and the low-field instrument was shown to be inadequate to detect the low 1,2 contents.

Monomer conversion after initiation (instantaneous monomer conversion denoted as p_A and p_B in Equations 4.13 - 4.15) is calculated directly from the absorbance values obtained at the specific wavelengths[19] for styrene and isoprene using a simple expression as follows:

$$\%\ Monomer\ Conversion = 100 * \frac{A_{initial} - A_t}{A_{initial} - A_{final}} \quad (4.16)$$

where $A_{initial}$ is the absorbance value at the time of initiation, A_t is the time dependent absorbance value and A_{final} is the final absorbance value at the point of complete depletion of the monomers. Monomer conversion can also be represented by Equation 4.17 (or Equation 4.15 in section 4.1 of this chapter) for styrene with $S(t)$ being the time dependent concentration of styrene monomer and S_0 being the initial styrene concentration:

$$p_S = 1 - \frac{S(t)}{S_0} \quad (4.17)$$

The instantaneous overall conversion can then be calculated as:

$$\%\ Overall\ conversion = (n_S * p_S) + (n_I * p_I) \quad (4.18)$$

where n_S and n_I are the initial mole fractions of styrene and isoprene.

Figure 4.5 presents plots of instantaneous overall conversions against the respective instantaneous monomer conversions for all the synthesized copolymers, which are representations of the compostional drifts for all copolymers. The instantaneous overall conversion versus instantaneous monomer conversion data (Figure 4.5) is curve-fitted to Equations 4.13 and 4.14

using the software, Kaleidagraph. To obtain the reactivity ratios of isoprene, r_I, the instantaneous unconverted styrene amount and the respective instantaneous overall conversion data are used (Equation 4.5). Analogously, the reactivity ratios of styrene, r_S, are obtained by utilizing the instantaneous unconverted isoprene amounts and the respective instantaneous overall conversion data. For both, the initial guess value for the reactivity ratios was set to 1 and the allowable was set to 0.1% in all cases. Table 4.2 lists the reactivity ratios and their products for all copolymers synthesized. It is significantly noticeable as to how the compositonal drifts tend to converge towards a flat-compositonal profile (the black line in all the compositional drift plots denotes a flat-compositional profile) going from pure cyclohexane to 50% TEA in the co-solvent mixture. This depicts the changing architecture of the copolymers as their solvent environment is varied, and achieving this was one of the primary goals of this project. Figure 4.6 presents the trends of compositional drifts of a) styrene and b) isoprene for all the copolymerizations carried out. This figure yet again shows how the drifts converge inwards towards the trend of random copolymerization (the black line) in which reactivity ratio products are equal to unity, as we move from 0% TEA towards 50% TEA.

Figure 4.7 and Table 4.2 shows that the r_I values decrease from 5.51 to 1.26 for 0 % TEA and 50 % TEA respectively. It can be concluded from this that varying TEA contents in the co-solvent mixture does have a pronounced effect on the copolymerization kinetics and monomer incorporation. Figure 4.8 shows how the copolymerizations going from pure cyclohexane to 50% TEA exhibit ideal copolymerization behaviour, i.e., the product of rectivity ratios gradually approximate unity at 50% starting from 0.77 at 0% TEA and approach randomness ($r_I = r_S = 1$).

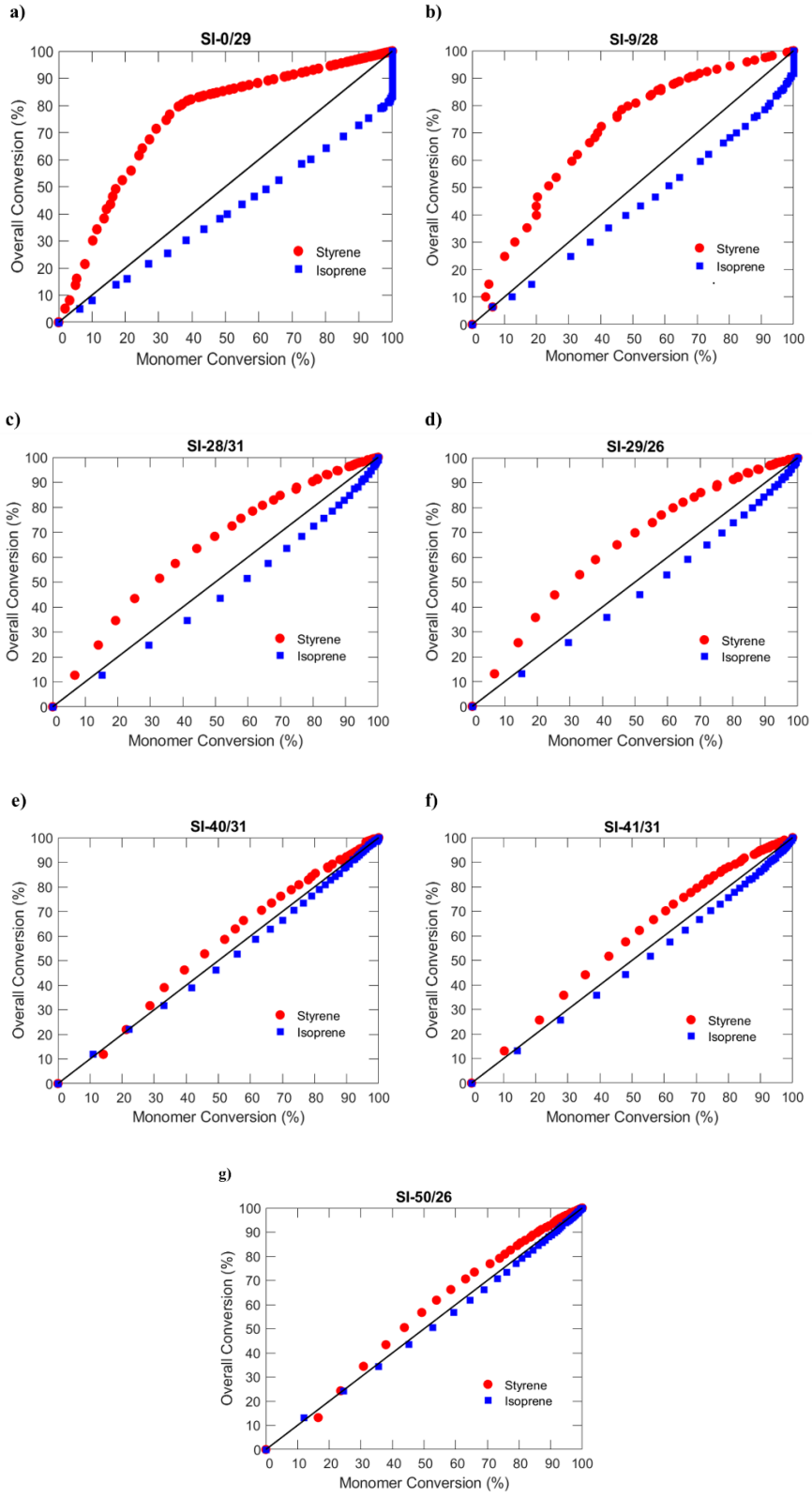

Figure 4.5 The instantaneous overall conversion plotted versus the instantaneous monomer conversion data (both styrene and isoprene) for all copolymers synthesized.

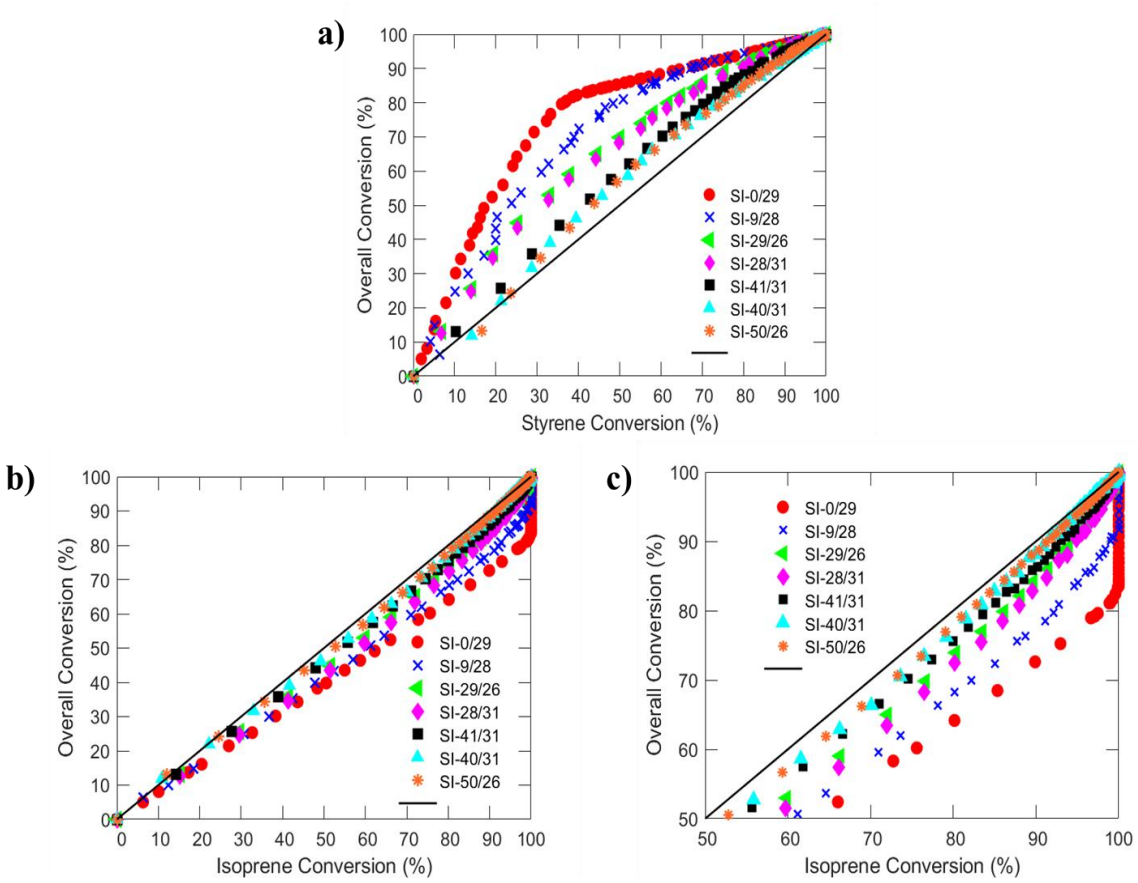

Figure 4.6 a) Styrene conversion data overlaid b) Isoprene conversion data overlaid c) A zoomed-in perspective of isoprene conversion data in for a greater visual clarity

Table 4.2 The reactivity ratios of all copolymers and their products

Polymer	r_I	r_S	r_I x r_S
SI-0/29	0.14	5.51	0.77
SI-9/28	0.26	3.37	0.88
SI-28/31	0.49	2.19	1.07
SI-29/26	0.48	2.19	1.05
SI-40/31	0.78	1.28	1.00
SI-41/31	0.67	1.49	1.00
SI-50/26	0.79	1.26	1.00

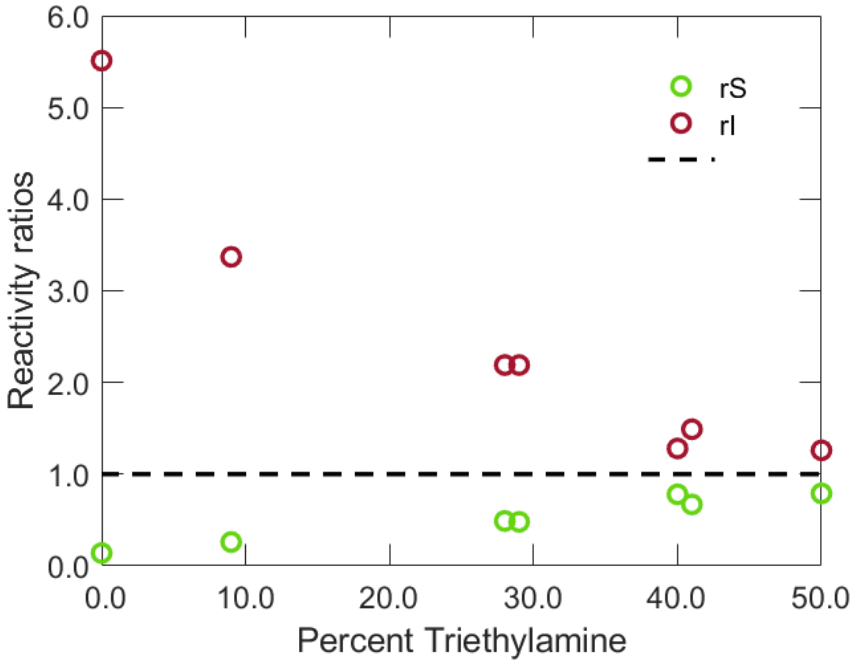

Figure 4.7 All the extracted reactivity ratios plotted against percent triethylamine in the solvent relative to the ideal copolymerization line (dotted).

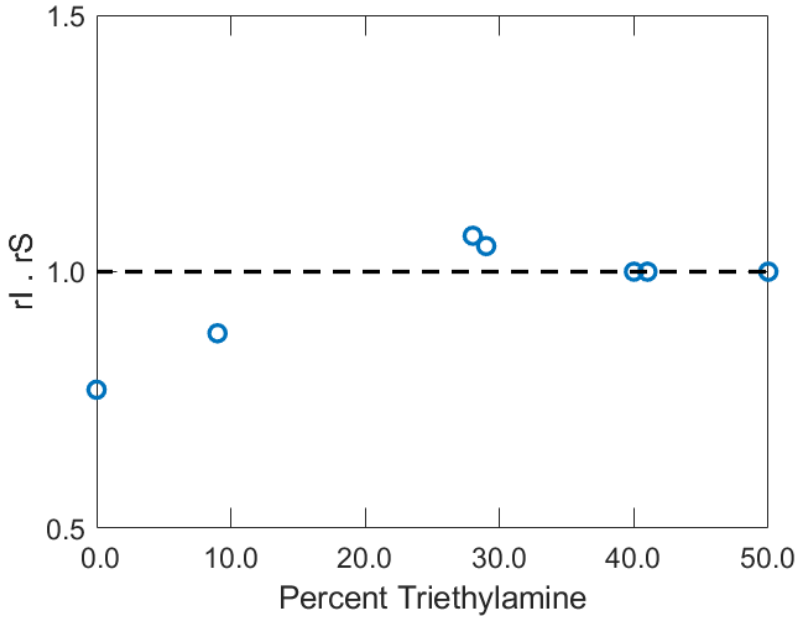

Figure 4.8 Product of reactivity ratios plotted against percent triethylamine in the solvent. The dotted line denotes the ideal copolymerization reactivity ratio product which is equal to unity.

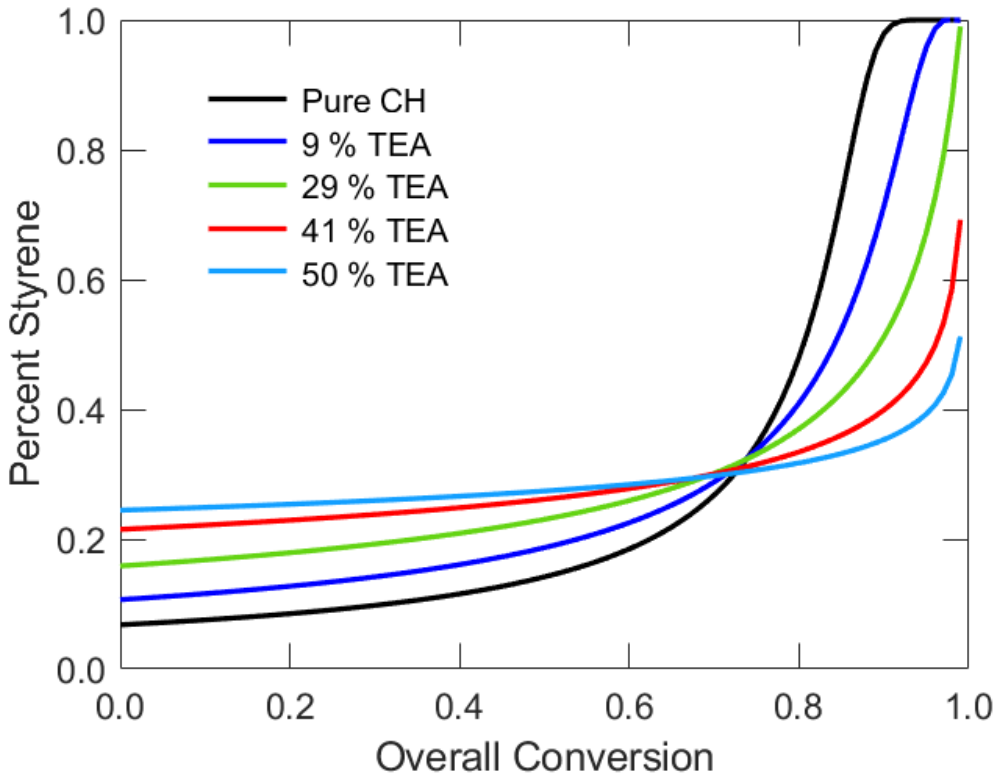

Figure 4.9 Instantaneous styrene percent in the copolymers plotted against the instantaneous overall conversions of the copolymerizations.

Figure 4.9 is a manifestation of the classical copolymer equation or Skeist Equation, Equation 4.3 (section 4.1), constructed using a constant initial styrene content of 29 mol % and using the reactivity ratios corresponding to different solvent conditions the variation in the compositional profile can be examined. As we can see from Figure 4.9, the styrene addition occurs at lower rates initially and increases rapidly as a majority of the isoprene is consumed. As the solvent composition approaches 50 % TEA, the styrene incorporation increases and the profile flattens out as a consequence of the changing relative reactivity.

4.4 Copolymer Characterization

4.4.1 Macromolecular characterization by Gel Permeation Chromatography (GPC)

Table 4.3 lists the molcular weights and the dispersities of the polymers synthesized. Half of the synthesized copolymers exhibit a narrow dispersity (< 1.1). All copolymers were analyzed as described in Chapter 2 (section 2.2.3). Copolymer samples were prepared at a concentration of 1 mg/mL in THF and the reported molecular weights are polystyrene-equivalent molecular weights.

Table 4.3 Copolymer macromolecular characterization by GPC

Polymer	**M_n (kg/mol)**	**$Đ = M_w/M_n$**
SI-0/29	8.8	1.12
SI-9/28	8.1	1.10
SI-28/31	5.5	1.08
SI-29/26	6.7	1.07
SI-40/31	7.6	1.11
SI-41/31	5.8	1.07
SI-50/26	8.7	1.11

4.4.1 Thermal Characterization by Differential Scanning Calorimetry (DSC)

The copolymers were analyzed using DSC to ascertain their glass transition temperatures. The T_g of polystyrene[20] varies depending on the molecular weight and that of polyisoprene[21] varies depending on the microstructure and molecular weight. After the equilibration at -80 °C, samples were heated at a rate of 10 °C min^{-1} to 150 °C and again cooled to -80 °C to erase the thermal history of the copolymers. At the same ramp rate of 10 °C min^{-1}, the samples are again heated to 150 °C to record the measurement of T_g.

It has been shown that a higher content of 1,4 units of isoprene causes a decrease in the T_g.[21] Here, a comparative analysis is complicated by the varied molecular weights, styrene contents and microstructure of the polyisoprene units. However, for each copolymer, the T_g anticipated for a random copolymer (one-phase system) can be calculated using the Fox equation[2]:

$$\frac{1}{T_g} = \frac{w_1}{T_{g1}} + \frac{w_2}{T_{g2}} \quad (4.19)$$

where, T_g is the glass transition temperature of the copolymer, w_1 and w_2 are the mass fractions of components 1 and 2 of the copolymer while T_{g1} and T_{g2} are the respective pure-component (homopolymer) glass transition temperatures. Using glass transition temperatures of polyisoprene reported by Widmaier and Meyer[21] as well as by calculating the glass transition temperatures of polystyrene using Equation 4.20, the expected T_g values were calculated for every copolymer which are listed in Table 4.4. The T_g values for all copolymers are also plotted versus the respective TEA contents that were used to synthesize them.

The glass transition temperature of the pure-component polystyrene based on its molecular weight can be calculated using the equation[22]:

$$T_g = T_{g,\infty} - \frac{K_g}{M_n} \quad (4.20)$$

where, T_g is the calculated glass transition temperature of polystyrene, $T_{g,\infty}$ is taken to be 100 (T_g of polystyrene of infinite molecular weight), K_g is a constant whose value has been experimentally determined to be 170,000 and M_n is the molecular weight of polystyrene whose glass transition temperature is to be calculated[22].

From Table 4.4, we see that the measured T_g values for the copolymers lie within a 5 °C deviation from the expected T_g values calculated using the Fox Equation (Equation 4.19) for all copolymers except SI-9/28 and SI-50/26 which show a very large deviation. All the DSC results are shown in Figure 4.10.

Table 4.4 Copolymer thermal characterization by DSC

Polymer	**Measured T_g (°C)**	**T_g (°C) (Polyisoprene)**	**T_g (°C) (Polystyrene)**	**Estimated Fox T_g (°C)**
SI-0/29	-45	-70	81	-41
SI-9/28	-12	-59	79	-33
SI-28/31	-15	-47	69	-20
SI-29/26	-21	-47	75	-24
SI-41/31	-16	-47	71	-20
SI-50/26	1	-47	81	-24

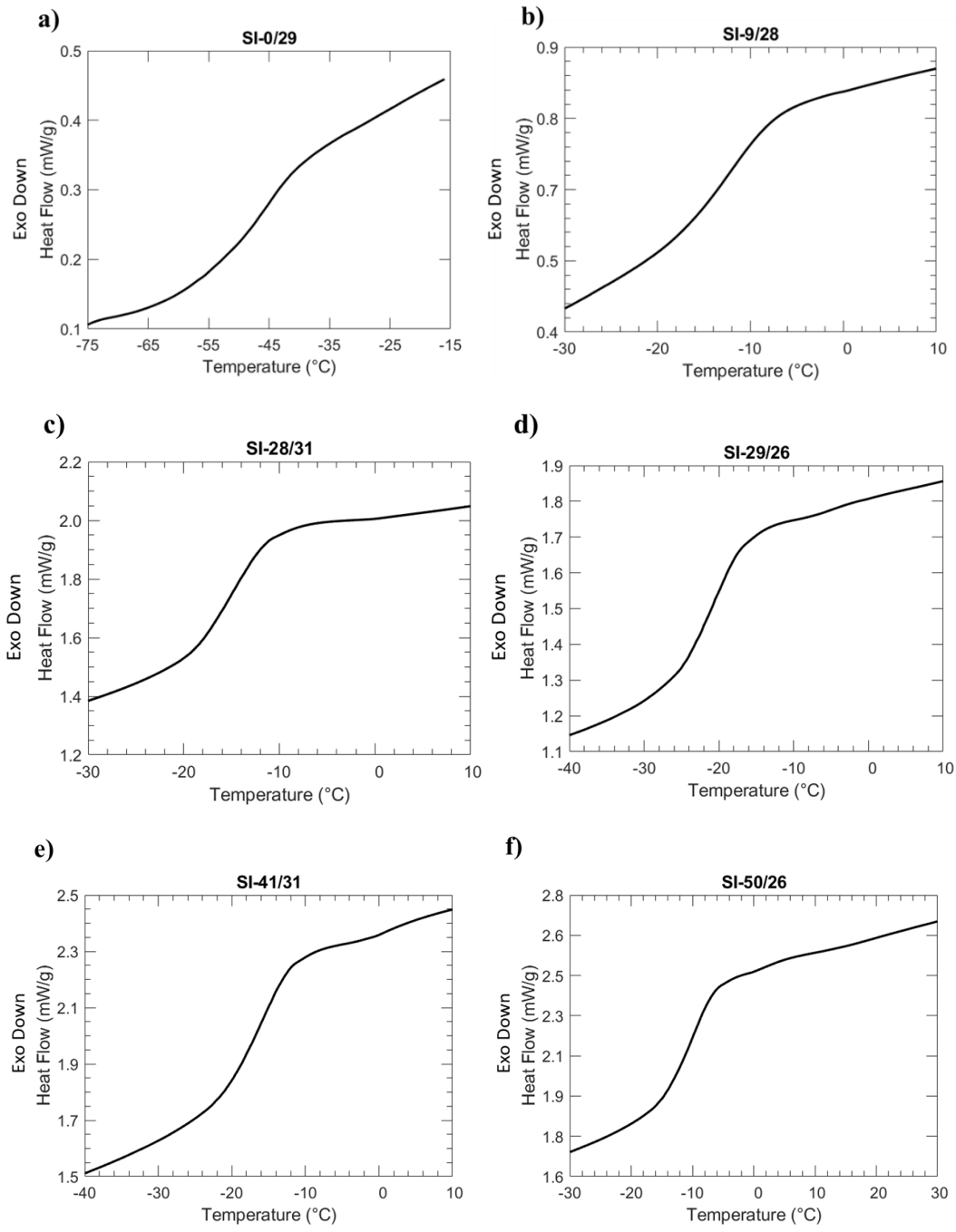

Figure 4.10 Results of thermal characterization by DSC.

4.5 Conclusions

ATR-FTIR spectroscopy has proved successful in aiding the tracking and analysis of the copolymerization kinetics of our specific copolymerization. We synthesize a spectrum of narrow disperse copolymers with distinct architectures, microstructure and compositional drifts by modifying the solvent environment systematically from a neat cyclohexane environment that gives rise to a high 1,4 content, block-like architecture to a 50/50 CH/TEA environment that gives rise a significantly more random distribution of styrene and isoprene units. The compositonal drifts tend to converge towards a flat-compositonal profile going from pure cyclohexane to 50% TEA in the co-solvent mixture, as shown in the literature. Thus, we herein demonstrated the ability to tune the copolymer architecture by varying the solvent environment, thus achieving one of the primary goals of this project. The 1,4 content of isoprene units is seen to decrease with the increasing content of TEA in the solvent mixture, while the content of 3,4 goes up. Copolymerization data incorporated to fit the classical copolymerization equation also fortified the monomer incorporation patterns that were anticipated (Figure 4.9).

4.6 References

(1) Beckingham, B. S.; Register, R. A. *Macromolecules* **2011**, *44* (11), 4313–4319.

(2) Sperling, L. H. *Introduction to Physical Polymer Science*, Fourth.; John Wiley & Sons, Inc., 2006.

(3) Odian, G. *Principles of Polymerization*, 4th ed.; John Wiley & Sons, Inc., New York, 2004.

(4) Beckingham, B. S.; Sanoja, G. E.; Lynd, N. A. *Macromolecules* **2015**, *48* (19), 6922–6930.

(5) Mayo, F. R.; Walling, C. *Chem. Rev.* **1950**, *46*, 191–287.

(6) Mayo, F. R.; Lewis, F. M. *Copolymerization. I. A Basis for Comparing the Behavior of Monomers in Copolymerization; The Copolymerization of Styrene and Methyl Methacrylate*; UTC, 1944; Vol. 66.

(7) Fineman, M.; Ross, S. D. *J. Polym. Sci.* **1950**, *5* (2), 259–262.

(8) Kelen, T.; Tudos, F. *J. Macromol. Sci. Part A - Chem.* **1975**, *9* (1), 1–27.

(9) Alfey, T.; Price, C. *J. Polym. Sci.* **1947**, *2* (1), 101–106.

(10) Song, J.; Hwang, E.; Lee, Y.; Palanikumar, L.; Choi, S. H.; Ryu, J. H.; Kim, B. S. *Polym. Chem.* **2019**, *10*, 582–592.

(11) Antkowiak, T. A.; Obesrster, A. E.; A. F. Halasa. *J. Polym. Sci. Part A Polym. Chem.* **1972**, *10*, 1319–1334.

(12) Chang, C. C.; Halasa, A. F.; Miller Jr, J. W.; Hsu, W. L. *Polym. Int.* **1994**, *33*, 151–159.

(13) Tierney, N. K.; Register, R. A. *Macromolecules* **2003**, *36*, 1170–1177.

(14) Wofford, C. F.; Hsieh, H. L. *J. Polym. Sci. Part A-1* **1969**, *7*, 461–469.

(15) Smith, S. D.; Ashraf, A.; J. Clarson, S. *Am. Chem. Soc.* **1993**, *34* (2), 672–673.

(16) Smith, S. D.; Ashraf, A.; Satkowski, M. M.; Spontak, R. J. *Am. Chem. Soc.* **1994**, *35* (1), 651–652.

(17) Hodrokoukes, P.; Pispas, S.; Hadjichristidis, N. *Macromolecules* **2002**, *35*, 834–840.

(18) Kelley, D. J.; Tobolsky, A. V. *Am. Chem. Soc.* **1959**, *81*, 1597–1600.

(19) Quinebèche, S.; Navarro, C.; Gnanou, Y.; Fontanille, M. *Polymer (Guildf).* **2009**, *50*, 1351–1357.

(20) Hitachi High-Tech Science Corporation. *DSC measurements of Polystyrene*; 1995.

(21) Widmaier, J. M.; Meyer, G. C. *Macromolecules* **1981**, *14* (2), 450–452.

(22) Bueche, F. *Physical Properties of Polymers*; New York: Wiley-Interscience, 1962; Vol. 199.

CHAPTER 5: CONCLUSIONS AND FUTURE WORK

5.1 Conclusions

This Thesis has explored the characterization and controlled synthesis of multicomponent polymer systems. The following sections discuss the core findings and propose future work related to this Thesis.

5.1.1 Low-Field ^{1}H-NMR Spectroscopy for Compositional Analysis of Multicomponent Polymer Systems

The utility of the low-field ^{1}H-NMR Spectroscopy for Polyisoprene microstructural characterization (to determine the % of 1,4 content) was put to test by running the synthesized polyisoprene sample with a high 1,4 content at varied number of scans (1, 2, 4, 8, 16, 64 and 128 scans) on the 60 MHz spectrometer and comparing the numbers so obtained with the 400 MHz spectrometer data acquired at 16 scans. An excellent agreement was obtained which fell within 1% (the confidence in compositional analysis performed using high-field NMR spectrometers in this manner for polymers is ±1%), between the 60 MHz and 400 MHz spectra. We therefore found the 60 MHz spectrometer capable of performing this characterization quantitatively as desired.

The commercial symmetric triblock compositional analysis results from the 60 MHz and 400 MHz NMR instruments were compared for SIS and SBS triblock copolymers. The result from the 60 MHz spectrometer fell within the typical experimental confidence for SIS while SBS was just outside with a 2% difference in composition. So, it could be said this level accuracy that comes with the 60 MHz spectrometer, keeping the lower cost and greater accessibility in perspective,

could be used for quality control, routine research and other applications after validation for specific systems of interest. The homopolymer blend compositional analysis for PS/PI and PS/PMMA blends yielded reliable data in favour of the 60 MHz spectrometer like in the other cases discussed above. For five of the nine PS/PI blends the compositions obtained using the 60 MHz spectra are equivalent to those from the 400 MHz spectra, after rounding to the nearest percent, with the remaining 4 differing by only 1%. Similarly, for PS/PMMA blends equivalent results are found for four of the nine blends, four differ by 1% and one differs by 2%. Overall, the average difference between the extracted compositions at 60 MHz and 400 MHz is 0.48% for PS/PI blends and 0.66% percent for PS/PMMA blends. These findings demonstrate the utility of low-field spectrometers for the quantitative determination of relative composition in these polymer blends.

Overall, ^{1}H NMR spectroscopy at low-field strength is a promising tool for the routine characterization of multicomponent polymer systems.

5.1.2 Tuning The Compositional Drift - Anionic Living Copolymerization of Styrene and Isoprene

In-situ ATR-FTIR spectroscopy has proved to be an efficient tool for the tracking and analysis of the copolymerization kinetics for our specific copolymerizations. Diverse narrow disperse copolymers of styrene and isoprene were synthesized with disparate architectures, microstructure and compositional drifts by modifying the solvent environment from a pure cyclohexane environment that gives rise to a high 1,4 content, block-like copolymer architecture to a 50/50 CH/TEA environment that produces a significantly more random distribution of styrene and isoprene units along the polymer chains (or a flat compositional profile in other words). The compositional drifts tend to flatten out going from pure cyclohexane to 50% TEA in the co-solvent mixture. Through the work in this thesis, we have established the ability to tune the copolymer architecture by varying the solvent environment, thereby acoomplishing the prime objective of this

project. The 1,4 content of isoprene units is seen to decrease with the increasing contents of TEA in the solvent mixture, while the content of 3,4 goes up as the TEA contents increase.

5.2 Future outlook

This section strives to present the additional work that could potentially be carried out as an extension of what has been accomplished thus far under each of these projects.

5.2.1 Low-Field ^{1}H-NMR Spectroscopy for Compositional Analysis of Multicomponent Polymer Systems

- Analysis of polymers of varying polyisoprene microstructures could be carried out and validated.
- There are various parameters associated with the experiments that can be conducted with the benchtop ^{1}H NMR spectrometer like number of scans (NS), O1 (Spectrometer Offset Frequency – Hz), P90 (90 degree pulse length – microseconds), RD (Recycle Delay between scans – seconds), Receiver Attenuation, Points to Acquire Per Scan, RFA0 (Transmit Pulse Amplitude).

  I would like to believe that an improved understanding of all of these parameters might help us set up wholesome ^{1}H NMR experiments that could give us the desired data by increasing the scope of measurement of the desired entities.
- By making use of the afore-mentioned understanding, it would be interesting to examine if the low-field ^{1}H NMR instrument can actually detect the 1,2 contents in polyisoprene.
- Validation of some more industrially significant polymer systems and subsequent contributions to literature would be another beneficial future prospect.

5.2.2 Tuning the Compositional Drift - Anionic Living Copolymerization of Styrene and Isoprene

- The effects of triethylamine contents between 0% and 9% as well as between 9% and 28% in the co-solvent systems on the compositional drifts could be examined in order to completely describe the co-solvent mixture system of triethylamine and cyclohexane between 0 % and 50 % TEA.
- Though the reactivity ratio values in pure cyclohexane indicate a clear preference for the isoprene monomer incorporation over styrene, the reason for a lower r_I value as compared to other analyses of this system[1,2] described in literature needs to be probed.
- Compositional drift data should be fit with other reactivity ratio models. Most notably, Meyer-Lowry analysis should be performed to corroborate the reactivity ratios found using the non-terminal model.[3]
- A long-term use of this capability would be the inclusion of different gradient structures within block copolymer architectures and to examine the impact on self-assembly behavior.

5.3 References

(1) Worsfold, D. J. *J. Polym. Sci. Part A-1 Polym. Chem.* **1967**, *5* (11), 2783–2789.

(2) Beckingham, B. S.; Register, R. A. *Macromolecules* **2011**, *44* (11), 4313–4319.

(3) Meyer, V. E., Lowry, G. G. *J. Polym. Sci*. **1965**, *3*, 2843–2851.